

DEVELOPMENT OF BIACORE PROTOCOLS FOR ASSESSING DNA  
BIOMOLECULAR INTERACTIONS

THESIS

Presented to the Graduate Council of  
Texas State University-San Marcos  
in Partial Fulfillment  
of the Requirements

for the Degree

Master of SCIENCE

by

Raul A. Puente, B.S.,

San Marcos, Texas  
August 2007

**COPYRIGHT**

by

Raul A. Puente

2007

## ACKNOWLEDGMENTS

I would like to begin by thanking GOD who has blessed me with a wonderful family and friends.

This pursuit for knowledge has been a beautiful experience. I have acquired more knowledge and experience through these two years than ever before.

I am thankful for the support my family has given me through these years I can not express in words my appreciation for your love and support, thank you for making me the person that I am now.

I have been blessed with great friends inside and outside the lab. Thanks to Robbie, Victoria, Memo, Isaac, Anita, Cristina, Daniel, and Sergio for their encouragement and friendship. I could not have asked for better friends to have during these two years. Victoria you have been a real trooper, you are an amazing person you have a great future ahead of you.

Last, but not least, I would like to extend my deepest appreciation to my committee: Dr. Lewis, Dr. Watkins, and my advisor Dr. David. Thank you Dr. Watkins and Dr. Lewis for offering valuable suggestions and improvements for the completion of this work. Thank you Dr. David for your guidance and patience, I enjoyed working in your lab.

This manuscript was submitted on May 16<sup>th</sup> 2007.

## TABLE OF CONTENTS

	Page
ACKNOWLEDGMENTS.....	iv
LIST OF TABLES .....	vii
LIST OF FIGURES.....	viii
CHAPTER	
I. INTRODUCTION .....	1
Base Excision Repair .....	1
UDG, SSB, and DNA polymerase $\beta$ .....	4
Uracil DNA Glycosylase (UDG) .....	4
Single Strand DNA Binding Protein (SSB) .....	5
DNA Polymerase $\beta$ .....	7
Surface Plasmon Resonance to Monitor Biomolecular Interactions.....	8
Project Outline .....	10
II. MATERIALS AND METHODS .....	14
Reagents .....	14
SDS-PAGE.....	14
Oligonucleotides and Proteins.....	15
Development of BIAcore Protocols.....	15
Instrumentation.....	15
Sensor Chips.....	18
Measurement of association/dissociation rate constants (kinetic analysis) .....	18
Immobilization and Binding Interactions.....	20
Immobilization of a model protein, Bovine Serum Albumin (BSA), on a carboxymethyl (CM5) chip .....	20
Biomolecular interaction analysis of BSA with Phenol Red and Warfarin .....	20
Immobilization of biotinylated oligonucleotides on Streptavidin (SA) chips .....	21

Generation of double-stranded DNA substrates.....	22
SDS-PAGE Analysis.....	22
Stability and Regeneration Studies .....	22
Stability of Derivatized chips.....	22
Regeneration of the sensor surface.....	23
DNA-Protein Interactions .....	23
Biomolecular Interaction Analysis.....	23
a) Formation of DNA Duplexes.....	24
b) Single Strand Binding (SSB) Protein.....	25
c) Uracil-DNA Glycosylase (UDG).....	25
d) Association of UDG with (SSB + DNA).....	25
e) DNA Polymerase $\beta$ .....	25
III. RESULTS AND DISCUSSION .....	27
General Protocols .....	28
Immobilization of a model protein.....	28
Immobilization pH-scouting .....	28
Interactions of BSA with Phenol Red and Warfarin.....	30
Immobilization of Biotinylated Oligonucleotides.....	32
Biomolecular Interactions .....	34
Formation of Normal and “Gapped” Duplexes <i>in situ</i> .....	34
DNA-Protein Interactions .....	37
DNA-Protein-Protein Interactions .....	41
Regeneration and Stability Protocols .....	44
Summary .....	48
REFERENCES.....	50

## LIST OF TABLES

<b>Table</b>	<b>Page</b>
1. Immobilization pH-scouting .....	29

## LIST OF FIGURES

<b>Figure</b>	<b>Page</b>
1. BER pathway (short-patch).....	3
2. Human uracil-DNA-glycosylase bound to DNA with a flipped uracil residue .....	5
3. Structure of E. coli SSB bound to single-stranded DNA .....	6
4. A ribbon structure of the ternary complex of rat DNA pol $\beta$ .....	7
5. Surface Plasmon Resonance phenomenon.....	9
6. Sensogram .....	10
7. Nucleotides containing the modified and the natural form of uracil.....	12
8. The BIAcore X system.....	16
9. Components of the BIAcore X.....	16
10. Successful derivitization of a CM5 sensor chip with BSA .....	29
11. Association/interaction of phenol red with immobilized BSA .....	31
12. Warfarin (250uM) injected over immobilized BSA .....	31
13. Immobilization of a biotinylated oligonucleotide (normal-ssDNA).....	32
14. Immobilization of a smaller amount of normal-ssDNA on a SA chip.....	33
15. Derivatization of a SA chip with abasic-ssDNA.....	33
16. Immobilization of pseudouridine containing ssDNA on a SA chip.....	34
17. Formation of a gapped duplex DNA .....	35
18. Hybridization of complementary DNA to form a normal-DNA duplex.....	36

19. Successful hybridization of complement DNA to form a normal-DNA duplex.....	36
20. Formation of an abasic duplex DNA (A) and surface regeneration (B) .....	37
21. Binding of SSB protein to single strand normal-DNA .....	38
22. Additional binding of SSB to single-strand normal-DNA .....	39
23. Binding of UDG to pseudouridine containing ssDNA .....	39
24. Protein-DNA interaction followed by surface regeneration .....	40
25. Formation of a gapped duplex DNA and binding by <i>X</i> pol $\beta$ .....	40
26. Interaction of UDG with binary complex (SSB-DNA).....	42
27. SDS-PAGE analysis of <i>X</i> pol $\beta$ and UDG .....	43
28. SDS-PAGE analysis of UDG.....	43
29. Protein-Protein-DNA interaction. ....	45
30. Interaction of Ethidium with a hairpin oligonucleotide .....	46
31. Determination of $K_D$ for ethidium/duplex DNA interaction.....	47

## CHAPTER 1

### INTRODUCTION

#### **Base Excision Repair**

DNA is constantly attacked by a variety of exogenous and endogenous agents (1). The lesions produced by these damaging agents lead to modifications of the DNA sequence which can lead to cancer. To maintain the structural integrity of DNA, cells have developed various defense mechanisms to prevent or repair damage and eliminate damaged cells (1-4). Therefore, investigation of these DNA repair mechanisms is an essential aspect of modern cancer research.

The base excision repair (BER) pathway is one of the defense mechanisms that cooperate to maintain integrity of the genome (1); it is an essential DNA repair pathway that repairs damage resulting from deamination, oxidation, and alkylation (2, 5). The BER pathway is responsible for correcting mismatches originating either from miscoding during replication/recombination or from spontaneous processes (6, 7) and is the most commonly employed repair mechanism to remove incorrect bases (8). Mutations resulting from miscoding are thought to be a major mechanism by which DNA-reactive agents cause disease such as cancer (1). Among the processes that constantly damage the DNA of all organisms, hydrolytic deamination of cytosine (C) to uracil (U) is the most frequent, occurring ~100-500 times per day in a human cell (2, 5, 9). If uracil residues

are not removed from DNA prior to replication, uracil will form base pairs with adenine producing a mutation of the original G:C base pair to an A:T base pair (10).

Reconstitution *in vitro* of the BER pathway indicates that repair may proceed via two alternative pathways termed “short-patch” and “long-patch” (1, 2, 7) with “short-patch” being the main pathway (Figure 1) (2, 8). In “short-patch” repair, the mechanism is initiated by DNA glycosylases (1, 2, 7, 8, 11). The DNA glycosylase recognizes the damaged bases and excises them from DNA by hydrolyzing the *N*-glycosidic bond between the base and the deoxyribose-phosphate chain to generate an abasic site (2, 6). The excision of the damaged base by the glycosylase produces an apurinic or apyrimidinic (AP) site (6) which is recognized and cleaved by action of the enzyme AP endonuclease producing a nick (1, 7). Repair of these AP sites is critical because they are unstable and cause mutagenesis and cell death (12). The nick produced by AP endonuclease is filled in by DNA polymerase  $\beta$  (pol  $\beta$ ) (1, 2, 6, 7). Subsequently, the nick is sealed by Ligase I (1, 2, 7).

In the proposed steps of the BER pathway for repair of uracil lesions, single-stranded DNA binding protein (SSB) may initiate the repair by binding to the uracil-containing DNA. Next, uracil-DNA-glycosylase (UDG) binds to the binary complex (DNA-SSB), removing uracil from the double helix and inserting the resulting extra-helical uracil residue into the active site (2, 3, 5, 11, 13). However, what is still not clear is exactly how UDG recognizes the mismatch and what protein-protein interactions might be involved. In this project we attempted to characterize the initial protein interactions involved in short-patch BER using surface plasmon resonance (SPR) technology developed by BIAcore, in particular utilizing the biosensor BIAcore X.

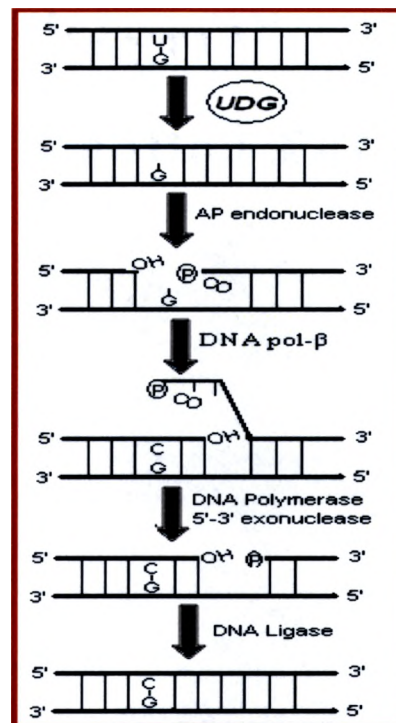


**Figure 1. BER pathway (short-patch).** Pathway of uracil excision by uracil-DNA-glycosylase (UDG).

Until now, most of the information suggesting the sequence of protein-protein interactions involved in the BER pathway has been obtained from pull down or activity assays (5, 9, 11). More recent investigations have started to integrate SPR technology to monitor in real-time these associations (13-16). For instance, Panayotou, *et al.* utilized a Biacore instrument to determine the efficiency of mutant UDG, mismatch-DNA glycosylase (MUG), and archeal DNA polymerase towards different substrates (single-stranded DNA and double-stranded DNA) containing uracil, successfully determining the affinity of these proteins towards their substrates (10). The results obtained by SPR technology correlate well with results previously obtained through methods other than surface plasmon resonance and illustrate the advantage of utilizing SPR over other methods- primarily, the ability to monitor the interaction as it occurs rather than just observe an end-product with no information of the intervening processes.

## **UDG, SSB, and DNA polymerase $\beta$**

### ***1. Uracil-DNA-Glycosylase (UDG)***

As previously mentioned, the presence of uracil in DNA occurs as a result of deamination of cytosine or by misincorporation (1, 6, 9, 13, 14, 16). UDG excises uracil from DNA and is the most specific and efficient DNA glycosylase (1, 2, 9, 13, 16, 17). UDG from *E. coli* was the first glycosylase to be discovered and characterized (1, 7) and it is used as a prototype to understand the biochemistry of uracil release (11). Subsequently, UDG enzymes from diverse biological sources have been purified (1, 18). Previous studies found significant amino acid similarity among several UDG enzymes including human-UDG, *E. coli* UDG, hsvUDG, and yeast-UDG (1, 5, 6, 18). The glycosylase utilized in this project was UDG from *E. coli* or eUDG. *E. coli* UDG is a monomeric protein of deduced MW ~25kDa, pI of 6.6, and 2-fold substrate specificity for uracil residues in single-stranded DNA over double-stranded DNA (18).

Crystal structures have demonstrated the mechanisms for the selective binding of uracil and the catalytic mechanism “pinch-push-pull” of UDG (Figure 2). The “base flipping” mechanism has been demonstrated as well by these crystal structures (1, 17). The 3-D structures of hUDG, HSV-1UDG, and eUDG are very similar (12). In the proposed UDG-uracil recognition mechanism, UDG scans the DNA by “pinching” the DNA backbone. When a mismatch is detected by UDG, the “pinching” mechanism creates a “kink” on the DNA backbone and this “kink” causes the base to “flip out” with the help of a push from the enzyme. Then as the base comes out of the double helix it is inserted into the active site of UDG and the *N*-glycosidic linkage is cleaved. The enzyme AP endonuclease cleaves the resulting AP-site-containing DNA strand (2, 5, 11).

The affinity of UDG for various substrates has been reported (2, 9, 11, 13, 18), and the results showed high preference of UDG for single-stranded (ss) DNA substrates over double-stranded (ds) DNA or gapped-DNA substrates. In addition, results suggested that UDG is carried to the site where the mismatch is located by the binary complex (DNA-SSB) (13).

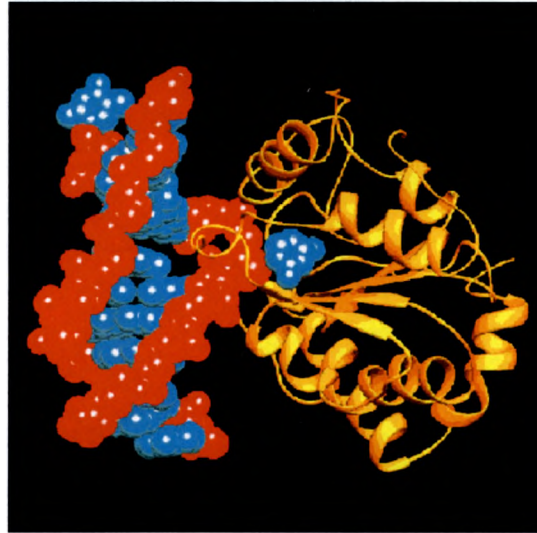


**Figure 2. Human uracil-DNA-glycosylase bound to DNA with a flipped uracil residue** (coordinates provided by C Mol and J Tainer) (19). In this figure the N-C1' glycosidic bond of the flipped nucleotide has been cleaved, and the free uracil is bound in the specificity pocket. DNA bases are shown in blue, sugar-phosphate backbone in red, and protein in gold.

## **2. Single Strand DNA Binding Protein (SSB)**

In general, SSB interacts with DNA and modulates several key processes such as replication, transcription, repair and recombination (11, 13, 14). Single-strand DNA binding protein (SSB) is a homotetramer consisting of monomeric (18.9 kDa) subunits of 117 amino acids (Figure 3). The secondary structure indicates that *E. coli* SSB can be divided into two parts: an *N*-terminal domain (~120 amino acids) which is rich in alpha-helices and beta-sheets and a *C*-terminal domain (~160 amino acids) that is more or less unstructured. The *N*-terminal two-thirds contain the DNA binding domain (13, 20). The

role of the *C*-terminal domain is still under investigation (13, 20); however it has been suggested the importance of the *C*-terminus is in the interaction of SSB with proteins in *E. coli* (13). Previous studies (3, 9, 11, 14) found that uracil is excised extremely poorly from dsDNA substrates containing a loop. This inefficient excision of uracil from dsDNA substrates suggested that destabilization (melting) of the DNA loop structures may be required for efficient repair (14). In fact, the presence of SSB lowers the  $T_m$  of these loop structures resulting in the melting ('unlocking') of the loop structures and allowing the formation of the productive enzyme-substrate complex. Interestingly, in a different study, results showed that when SSB is bound to ssDNA the excision activity of UDG decreases (11). These findings suggest that SSB may facilitate the recruitment of UDG to the site of the uracil-containing lesion by serving as a carrier (13). SSB utilized in this project was from *E. coli*.

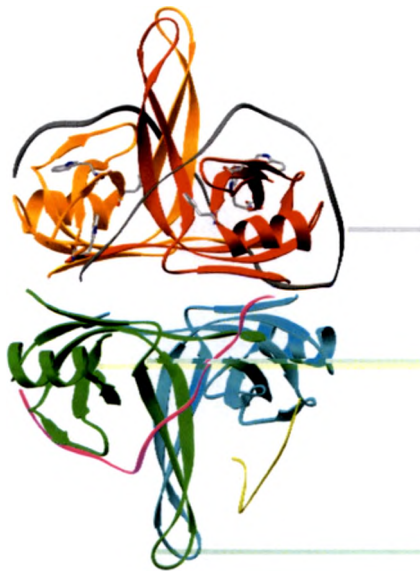


**Figure 3. Structure of *E. coli* SSB bound to single-stranded DNA** (coordinates provided by Waksman, G. *et al*) (21). The structure of the DNA binding domain of the single-stranded DNA binding protein from *E. coli* (Eco SSB) bound to two 35-mer ssDNAs was determined to a resolution of 2.8 Å. This structure describes the vast network of interactions that results in the extensive wrapping of ssDNA around the SSB tetramer and suggests a structural basis for its various binding modes.

### 3. DNA Polymerase $\beta$

DNA polymerases *in vivo* play a central role in several DNA transactions including a gap-filling synthesis role during base excision repair (BER) (3, 4, 15, 22). The DNA polymerase  $\beta$  (DNA pol  $\beta$ ) is the smallest of the four nuclear DNA polymerases ( $\alpha$ ,  $\beta$ ,  $\gamma$ , and  $\epsilon$ ) (3, 4). DNA polymerase  $\beta$  is a highly conserved 39 kDa protein (335 amino acids) consisting of two domains, a 31 kDa C-terminal domain that includes the polymerase active site and an 8 kDa N-terminal domain that participates in binding to DNA (4, 15, 22) (Figure 4 shows the ribbon structure of rat DNA pol  $\beta$  (4)).

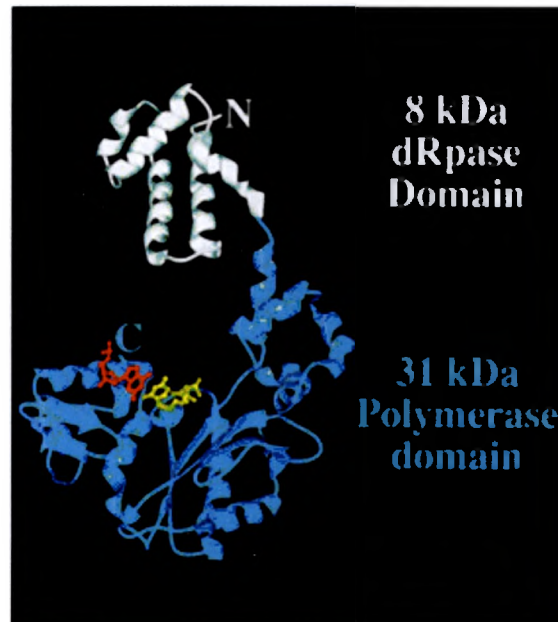


**Figure 4.** A ribbon structure of the ternary complex of rat DNA pol  $\beta$ . The structure shows the positions of the cleaved nucleotide (in red) and the incoming correct nucleotide (in yellow).

Previous studies have provided extensive information on the structure-function relationship of the DNA pol  $\beta$  complex (4, 15). It has been reported that the 8 kDa domain has a high affinity for ssDNA, whereas the C-terminal 31 kDa domain binds to

dsDNA weakly and has catalytic activity (3, 4, 15, 22). The affinity of DNA pol  $\beta$  for dsDNA containing nicks bearing the 3' ends of upstream primers and the 5' termini of downstream primers, as well as the preference of DNA pol  $\beta$  to bind to both the template and primer strands has been reported (3, 15, 22). However, DNA pol  $\beta$  possesses higher affinity for ssDNA substrates over dsDNA substrates, with  $K_A$  values for ssDNA ( $1.25 \times 10^8 \text{ M}^{-1}$ ) about 2-fold higher than for dsDNA ( $7.56 \times 10^7 \text{ M}^{-1}$ ) (15). These differences in binding were attributed to the differences in the binding modes of DNA pol  $\beta$  to DNA substrates. Both domains (*C*- and *N*-terminal) bind to ssDNA, whereas for dsDNA only the *C*-terminal domain binds to the DNA substrate. In the same study Tsoi, *et al.* (15) reported that DNA pol  $\beta$  binds to gapped dsDNA substrate with similar kinetic rate and affinity constants as for blunt-ended dsDNA. However, the region to which DNA pol  $\beta$  binds to is still not clear.

DNA polymerase- $\beta$ , aside from its catalytic function, interacts with proteins known to be involved in the BER pathway including AP endonuclease and DNA ligase I suggesting sequential coordination (3).

Recombinant *Xiphophorus* pol  $\beta$  shares greater than 80% sequence homology with mammalian DNA pol  $\beta$  and exhibits identical size and nearly identical activity to its human counterpart (23). Recombinant *X*pol  $\beta$  was utilized in this study.

### **Surface Plasmon Resonance to Monitor Biomolecular Interactions**

The development of surface-plasmon-resonance (SPR) biosensors has made kinetic analysis of most biomolecular interactions accessible by allowing monitoring real-time analysis of reactions without the use of labels. Since their introduction in 1990 many Biacore models have become commercially available (24).

The Biacore systems use a highly specialized optical technique to monitor changes in the refractive index in the vicinity of a surface. To perform analyses in a Biacore system, a reactant (*ligand*; Biacore terminology) needs to be immobilized on a surface in order to monitor its interaction with a second component (*analyte*; Biacore terminology) in solution (25). The Biacore systems comprise 1) an SPR detector, 2) a sensor chip, and 3) an integrated liquid handling system for the exact transport of the sample to the adsorption and detection spot (25).

Binding studies using an SPR biosensor have contributed significantly to the understanding of the molecular basis of biomolecular interactions (14). In the Biacore X system, the SPR detector records changes in refractive index near the sensor surface (Figure 5) and translates these changes into a detectable signal (a sensogram) (Figure 6) (26).

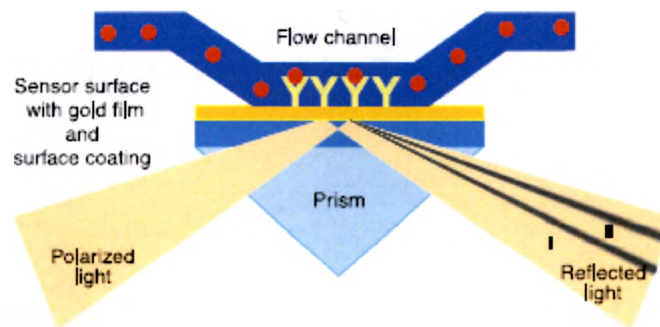


**Figure 5. Surface Plasmon Resonance phenomenon.** In the Biacore X system, light is directed at, and reflected from the side of the sensor surface not in contact with sample. The light is reflected at a specific combination of angle and wavelength (refractive index). As molecules bind to the sensor surface, the refractive index is affected and it changes producing a SPR signal. This change in refractive index is detected and the SPR signal is expressed in resonance units (RUs). One RU is approximately equivalent to one picogram per square millimeter on the sensor surface.

The sensogram represents the biospecific interaction between an immobilized molecule (*ligand*) and a binding partner (*analyte*) (14). The sensogram produced is proportional to the mass of molecules that bind to the surface and can be monitored continuously (26). This technology has been applied to multiple biomolecular interaction studies involving a variety of molecules of low- and high-molecular weight.

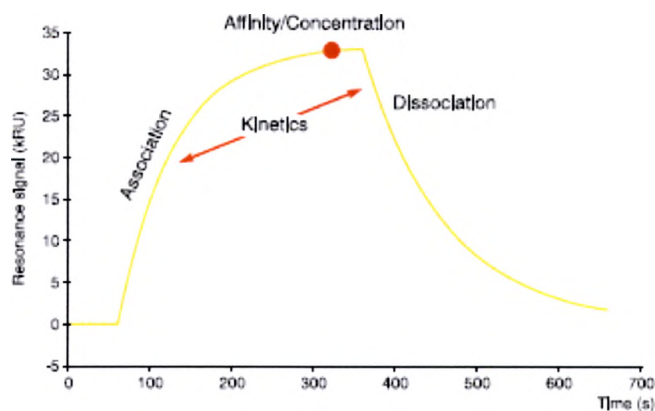


**Figure 6. Sensogram.** The signal produced during the association and dissociation events during a binding analysis. The change in refractive index is detected by the instrument and translated into a sensogram.

### Project Outline

The major goal of this project was to characterize important parameters for monitoring both enzyme-substrate recognition and protein-protein interactions in BER through biospecific interaction analysis (BIA) using the biosensor Biacore X.

Recently, SPR systems developed by Biacore have been used in several studies (13-16) to monitor the binding events of several proteins in the BER pathway. The biosensor Biacore X is an ideal system to carry out this study; it is highly sensitive, allows the study of samples ranging from small molecules to large surface complexes,

and is able to monitor rapid associations/dissociations. BIAcore X uses small amounts of sample to monitor binding events.

The primary advantage of the BIAcore X for the purpose of this project is its detection range. Affinities ( $K_A$ ) in the ranges of  $10^5 - 5 \times 10^{11}$  1/M,  $k_a$  in the ranges of  $10^3 - 5 \times 10^6$  1/M · s, and  $k_d$  in the ranges of  $10^{-5} - 10^{-2}$  1/s can be determined using the BIAcore X (BIAcore instrument handbook). Previous studies using various BIAcore systems have reported kinetic information for DNA-binding proteins. The kinetic values reported are within the detection ranges of our biosensor BIAcore X. For instance, Panayotou, *et al.* reported the on and off rates as well as substrate affinity of a mutant form of UDG. The results showed preference of the mutant UDG for ssDNA substrates. The reported  $K_D$  values for ssDNA and dsDNA substrates were 4.65 nM and 57.4 nM, respectively (10). Interactions between SSB and UDG from *E. coli* and *Mycobacteria* have also been characterized. The  $K_D$  values for interaction between *E. coli* SSB/UDG and *Mycobacteria* SSB/UDG were  $1.70 \times 10^{-7}$  M and  $1.40 \times 10^{-7}$  M respectively; no  $K_D$  value was obtained for the *E. coli*/*Mycobacteria* SSB/UDG interactions (9). Tsoi, *et al.*, utilizing a BIAcore X, reported affinity values of human pol  $\beta$  for different substrates (15). The  $K_A$  for ssDNA and gapped DNA substrates were  $1.25 \times 10^8$  1/M and  $0.85 \times 10^8$  1/M, respectively. These results indicated greater affinity of human pol  $\beta$  for ssDNA than for gapped-DNA (15).

Prior to analysis of DNA-protein interactions we established immobilization protocols for the desired substrates (*ligands*) on the BIAcore X system. In order to determine optimal conditions for binding analysis, we utilized Bovine Serum Albumin (BSA) as a model *ligand* and phenol red and warfarin as *analytes*. Bovine serum albumin

was used as a model protein because it is well-characterized and it is readily available. The dye phenol red and the compound warfarin were used because they have been previously reported to have relatively high affinity for albumin (27).

In order to characterize binding of proteins from the BER pathway to their substrates, different forms of DNA substrates were utilized: single-stranded biotinylated oligonucleotides that were either a non-specific substrate, an oligonucleotide containing an abasic site, or an oligonucleotide containing a modified form of uracil (pseudouridine base ( $\Psi$ dU) a substrate mimic) and double-stranded oligonucleotides (a blunt-end duplex and a gapped duplex). We utilized an oligonucleotide containing a non-natural substrate ( $\Psi$ dU) (Figure 7) for UDG because the natural (Figure 7) removal of uracil from DNA by UDG occurs at a rate so fast (rate acceleration  $\sim 10^{12}$ ) (2) that it would not be detected by the biosensor. As reported by Parikh *et al.* (28) this particular substrate (2'-deoxypseudo-uridine (d $\Psi$ U)) is processed similarly to uracil but it is not cleaved by UDG. The association of pol  $\beta$  with a gapped duplex was predicted to occur readily.

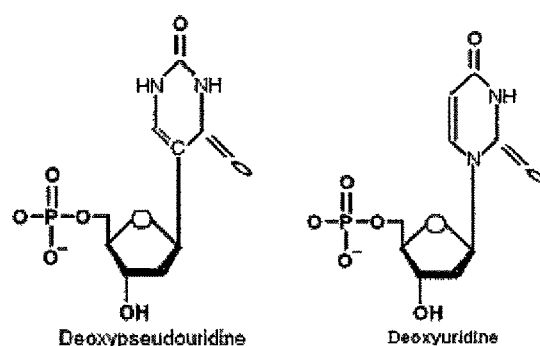


**Figure 7. Nucleotides containing the modified and the natural form of uracil. Deoxypseudouridine and Deoxyuridine.**

For protein-protein interaction analysis, we chose *E. coli* UDG and SSB. These proteins have already been reported to be involved in the initial stages of the BER

pathway (2, 29) and they have been both used in recent binding studies using Biacore technology (7, 10, 13, 14). The interaction between these proteins and selected substrates was monitored to investigate enzyme-substrate recognition and protein-protein interactions.

In summary, in order to characterize parameters necessary for observing the initial sequence of the BER pathway by SPR, we attempted to establish immobilization protocols and conditions that would allow for optimal binding using the biosensor BIAcore X. The information obtained from this study can be useful for future binding studies.

## CHAPTER 2

### MATERIALS AND METHODS

#### 1. Reagents

All chemicals were reagent grade and purchased from Sigma-Aldrich (St. Louis, MO) unless otherwise noted. Phenol red was purchased from Matheson Coleman & Bell. Running buffer HBS-EP (0.01 M HEPES pH 7.4, 0.15 M NaCl, 3 mM EDTA, 0.005% v/v Surfactant P20); 10 mM sodium acetate (pH 4.0, 4.5, 5.0, and 5.5); (1-ethyl-3-(3-dimethylaminopropyl)carbodiimide hydrochloride (EDC); *N*-hydroxysuccinimide (NHS); 1.0 M ethanolamine (pH 8.5); 10 mM glycine hydrochloride (pH 2.5); and 0.1% sodium dodecyl sulfate (SDS) were purchased from BIAcore (GE Healthcare, Piscataway, NJ). Magnesium chloride (MgCl<sub>2</sub>), (unknown source). NaOH/NaCl (50mM/0.5M) was used to activate the sensor surface of streptavidin (SA) chips.

#### **SDS-PAGE:**

Tris base, NuPAGE® Novex 10% Bis-Tris Gels, SeeBlue® Pre-Stained Standard, SimplyBlue™ SafeStain, NuPAGE® LDS Sample Buffer (4X), NuPAGE® Reducing Agent (10X), NuPAGE® Antioxidant, and MOPS Running Buffer were purchased from Invitrogen Life Technologies (Carlsbad, CA).

### **Oligonucleotides and Proteins:**

Biotinylated oligonucleotides obtained from Integrated DNA Technologies, Inc. (Coralville, IA) include the following: 5'-GTG TAC GTT AAC GGA TCC CCG GGT ACC GAG C/3BioTEG/-3' (labeled 'normal' strand); 5'-GTG TAC GT/idSp/ A ACG GAT CCC CGG GTA CCG AGC /3BioTEG/ -3' (labeled 'abasic' strand); 5'-GCT CGG TAC CCG GGG ATC CGT TAA CGT ACA C-3' (labeled 'complementary DNA strand'); 5'-TCC GTT AAC GTA CAC-3' (labeled 'upstream'); 5'GCT CGG TAC CCG GGG-3' (labeled 'downstream'); and a 5'- biotinylated hairpin-forming oligonucleotide of sequence 5'-BioTEG/- CGG CCT CCC CAG GCC G – 3'. A biotinylated pseudouridine-containing oligonucleotide of the following sequence, 5'- GTG TAC GTpU AAC GGA TCC CCG GGT ACC GAG C (Biotin-TEG) 3', was obtained from TriLink BioTechnologies (San Diego, CA).

The following proteins were used without further purification: Uracil-DNA-Glycosylase (UDG, Invitrogen, 100U (1U/□l) activity units), Single Strand Binding Protein (SSB, Sigma-Aldrich in 20 mM Tris-HCl, pH 8.0, 0.5 M NaCl, 0.1 mM EDTA, 0.1 mM DTT, and 50% glycerol), Bovine Serum Albumin (BSA, Sigma) and *Xiphophorus* recombinant DNA polymerase  $\beta$  ( $X_{pol} \beta$  courtesy of Dr. Ron Walter, Molecular Bioscience Research Group, Department of Chemistry & Biochemistry, Texas State University-San Marcos).

## **2. Development of BIAcore Protocols**

### **A. Instrumentation**

The BIAcore X system was manufactured by BIAcore (GE Healthcare, Piscataway, NJ) (Figure 7).



**Figure 8. The BIAcore X system.**

The BIAcore X system contains an optical detector system, a removable sensor chip, and a microfluidic cartridge which controls the injection of samples onto the sensor chip surface (Figure 8).

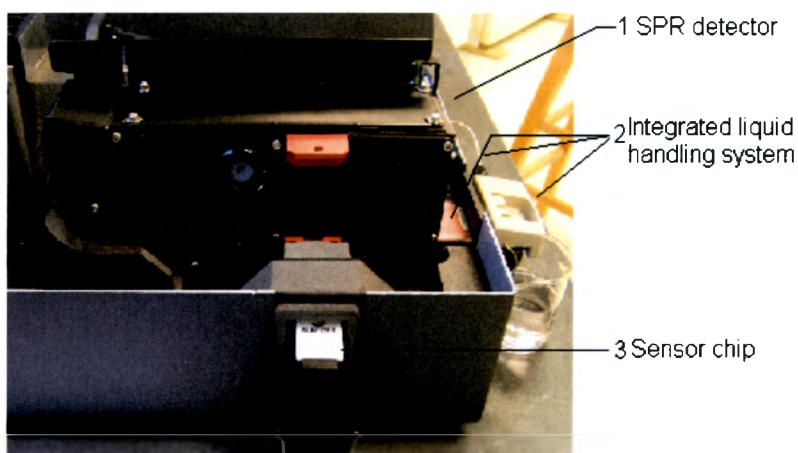


**Figure 9. Components of BIAcore X.** The BIAcore comprises 1) an SPR detector, 2) an integrated liquid handling system (liquid delivery pump and Integrated  $\mu$ -Fluidic Cartridge (IFC)), and 3) a sensor chip.

The instrument is controlled by a personal computer with dedicated software and a BIAevaluation data processing program. Sensor chips consist of a glass slide coated on one side with a thin gold film to which is attached a dextran layer derivatized with a biomolecule of interest. The immobilized biomolecule is termed the “**ligand**”.

A microfluidic cartridge holds the sensor chip in contact with a prism that is part of the optical system. A buffered sample (termed the “**analyte**”) is introduced into the injector loop and flows over the sensor chip. The prism focuses polarized light into a transverse wedge which hits the glass-gold interface, and the reflected light is detected by a two-dimensional array of photodiodes which measure its change in intensity. A change in composition and mass at the dextran-gold interface leads to a change in the refraction angle of reflected light that is measured. This shift in angle ( $\Delta R$ ) is continuously monitored and expressed as a sensogram (24, 30). To eliminate small “bulk” refractive index change differences at the beginning and end of each injection (due to small differences in buffer composition of analyte solutions) a control sensogram obtained over a nonbinding surface is subtracted for each analyte injection.

The development for biomolecular interaction analysis (BIA) has allowed the monitoring of a wide range of molecular reactions in real-time by surface plasmon resonance (SPR) providing qualitative and quantitative information. For example, the interaction affinity between UDG and SSB from two different systems was characterized using BIAcore technology, as well as the domain from SSB that interacts with UDG (13). Protein-DNA interactions have also been observed, including the formation of the lac repressor-operator complex at various concentrations using a BIAcore system (26). Antibody-antigen binding has been the most widely-studied biomolecular interaction; in fact the interaction of prostate-specific antigen (PSA) with monoclonal antibody (mAB) was used to validate the reliability of BIAcore technology (31).

### **Sensor Chips:**

A sensor chip is a glass slide coated with a thin gold film to which a surface dextran matrix is covalently bonded. The matrix surface forms one wall of the detector flow cell. The chips utilized in this study were of the type CM5 (carboxymethyl dextran) and SA (streptavidin) research grade. The CM5 chips are typically used to immobilize proteins or other ligands containing an amino functionality. Ligands remain covalently attached to the dextran surface after immobilization. The SA chip contains a dextran matrix to which streptavidin has been covalently attached, so the surface is prepared for high affinity capture of biotinylated ligands (24). Streptavidin has a high affinity for biotin ( $K_D \approx 10^{-15}$  M) and the interaction can not be easily removed (32).

### **Measurement of association/dissociation rate constants (kinetic analysis):**

The refractive index within the dextran matrix is continuously monitored, plotted against time, and presented in a sensogram. The molecular interaction response is measured in resonance units (RU). For most proteins and DNA, 1000 RU corresponds to a surface concentration of approximately  $1\text{ ng/mm}^2$ . Detailed descriptions of kinetic analysis of biomolecular interactions have been published (26, 30). A brief theoretical background is presented here.

During association, the free concentration of analyte may be considered constant and identical to the total concentration because during injection of the analyte over the sensor surface, the analyte solution is constantly replenished. The interaction between the ligand and the analyte can therefore be assumed to follow pseudo-first-order kinetics described by the following equation:

$$\begin{aligned}
 dR/dt &= k_a(R_{\max} - R)C - k_dR \\
 &= k_aR_{\max}C - (k_aC + k_d) R, \quad (\text{Eq. 1})
 \end{aligned}$$

where  $dR/dt$  is the rate of surface complex formation,  $R_{\max}$  is the maximum binding capacity of the immobilized ligand,  $R$  is the amount of analyte bound to immobilized ligand, and  $C$  is the concentration of the flowed analyte.

In principle,  $k_a$  can be obtained by plotting the slope of  $dR/dt$  versus  $R$  (expressed in RU) against the concentration of analyte,

$$\text{slope}(dR/dt \text{ vs } R) = k_aC + k_d \quad (\text{Eq. 2})$$

This equation gives a new line from which the association rate constant is obtained as the slope of the line. When the sample (analyte) pulse has passed the surface and is replaced by running buffer, the concentration,  $C$ , of free analyte suddenly drops to zero. At this point, the contribution to  $C$  by dissociated analyte will be insignificant. The rate equation now is

$$\begin{aligned}
 dR/dt &= -k_dR, \\
 \ln R_{t1}/R_{tn} &= k_d (tn-t1) \quad (\text{Eq. 3})
 \end{aligned}$$

where  $R_{t1}$  is the relative value of resonance in RU at time  $t1$  and  $R_{tn}$  is that at time  $tn$ . The relative RU indicates the increase in the RU value relating to the baseline RU value obtained in the hybridization buffer alone.

The equilibrium affinity constant ( $K_a$ ) is calculated from association and dissociation rate constants ( $k_a/k_d$ ).

## **B. Immobilization and Binding Interactions**

### **Immobilization of a model protein, Bovine Serum Albumin (BSA), on a carboxymethyl (CM5) chip:**

Following is a representative protocol for BSA immobilization on the surface of a CM5 sensor chip. The sensor chip (CM5) was primed (equilibrated) with running buffer HBS-EP (0.01 M HEPES pH 7.4, 0.15 M NaCl, 3 mM EDTA, 0.005% v/v Surfactant P20) + 3% DMSO. Next the sensor surface was activated with a 70  $\mu$ l injection of a mixture of equal volumes consisting of *N*-hydroxysuccinimide (NHS, 0.1 M) and *N*-ethyl-*N*-(3-diethylaminopropyl)-carbodiimide (EDC, 0.4 M). Finally, an aliquot of 70  $\mu$ l of BSA solution (typically, 1 mg/ml in 10 mM sodium acetate at pH 5.0) was injected over flow channel 2 (Fc2) producing the desired immobilization response (typically ~2300 response units (RU); this value indicates that about 2.0 ng/mm<sup>2</sup> of the BSA have been captured by the carboxymethylated dextran matrix). Finally, an injection of ethanolamine (70  $\mu$ L) was performed to block any remaining activated ester groups on the sensor chip surface. The flow rate during this immobilization procedure was typically set at 10  $\mu$ l/min. For the amount of immobilized BSA indicated above, the maximal response that can be expected upon binding of a small molecular weight ligand such as warfarin is 10 RU's, assuming 100% of the binding sites are occupied.

### **Biomolecular interaction analysis of BSA with Phenol Red and Warfarin:**

The association of phenol red and warfarin with immobilized BSA was monitored according to the following procedures: Aliquots of phenol red (55  $\mu$ l) diluted in buffer (10 mM sodium acetate pH 5.5) at various concentrations ( $4 \times 10^{-6}$  –  $8 \times 10^{-6}$  M) were injected at a constant flow rate over the BSA-immobilized and reference surfaces.

Aliquots of warfarin (50  $\mu$ l of 450 nM - 250  $\mu$ M) solutions in 3% DMSO solution were similarly injected over the BSA and reference surfaces. After each injection, a pulse of running buffer was performed to elute any remaining bound analyte and reestablish a baseline for the sensor chip surface. All injections of phenol red and warfarin were performed at a flow rate of 5  $\mu$ l/min.

The apparent stoichiometry and maximal response of the surface complex was calculated from the saturating binding capacity of the surface by the equation:

$$R_{MAX} = R_L \times (MW_A/MW_L) \times S \quad (\text{Eq. 4})$$

where  $MW_A/MW_L$  is the ratio of molecular weight of analyte (A) to ligand (L),  $R_L$  is the amount of ligand bound to the sensor surface in RU, and S represents the stoichiometry of analyte to ligand.

#### **Immobilization of biotinylated oligonucleotides on Streptavidin (SA) chips**

For the derivatization of streptavidin (SA) chips, the desired 3'-biotinylated oligonucleotides were utilized. Each oligonucleotide was diluted to 100  $\mu$ M in HBS-EP buffer for indefinite storage at -20°C. Prior to immobilization the oligonucleotide was typically diluted to 1-10 nM in running buffer. The streptavidin matrix surface of SA chips was prepared for immobilization by washing with running buffer (HBS-EP) for 5-10 minutes at a constant flow rate 50  $\mu$ l/min followed by short injections of NaOH/NaCl (50 mM / 0.5 M) solution. Next, aliquots of the diluted oligonucleotide were injected until the desired RU response was reached. Finally, the derivitized binding surface was washed with pulses of running buffer to remove any unbound oligonucleotides. The amount of biotinylated oligonucleotide immobilized can be controlled by adjusting 1) the

concentration of the injection solution, 2) the injection volume, and 3) the injection time. The difference of the signal before and after the injection of oligonucleotide determined the actual amount (in RU) of oligonucleotide immobilized.

#### **Generation of double-stranded DNA substrates:**

To produce double-stranded oligonucleotide ligands, non-biotinylated complementary oligonucleotides were hybridized *in situ* to the immobilized biotinylated ligands. The formation of the double-stranded molecule was verified by observing the response during the injections of the non-biotinylated oligonucleotides; doubling of the response units (RU) was an indication of the formation of a duplex. If too much of the non-biotinylated oligonucleotide was injected, the response would reach a saturation level and no additional hybridization was detected. To remove weakly bound material, a washing procedure with running buffer (HBS-EP) was performed several times after immobilization and prior to any binding analyses.

#### **SDS-PAGE Analysis:**

Two samples of UDG and *Xpol*  $\beta$  were prepared, each containing: 5  $\mu$ l of UDG or *Xpol*  $\beta$ , 2.5  $\mu$ l of loading buffer, 1  $\mu$ l of reducing agent, and 1.5  $\mu$ l of deionized water, and were loaded on 10% Bis-Tris precast gels which were used as recommended by Invitrogen, except that gels were run for 54 minutes at 200V.

### **C. Stability and Regeneration Studies**

#### **Stability of Derivatized chips:**

The stability of immobilized sensor chips is important in this type of analysis because repetition of binding studies can be done on the same chip only if the sensor surface remains the same. Stability of the chips was usually determined after the chip was

first immobilized, exposed to binding analysis, and subsequently regenerated. If the chip surface was stable (good), continuous associations could be performed after regeneration procedures. Sensor chips were stored either dry or in buffer at 4°C.

In order to test for stability of the oligonucleotide immobilized chips, the efficiency of binding to SSB or the corresponding complement was assessed. Single strand binding protein (SSB) proved to be a very reliable analyte to test for the stability of the sensor surface. When a chip had been degraded, no further binding association with SSB was detected.

### **Regeneration of the sensor surface:**

In every case after binding of analyte to a ligand-immobilized sensor chip, regeneration of the sensor surface was performed to reestablish the original baseline response. Solutions of 0.1% SDS, glycine pH 2.5, 1 M NaCl, or 0.5% DMSO (depending on the analyte bound to the ligand) were injected in small volumes, typically 5  $\mu$ l -10  $\mu$ l, at a slow flow rate, (5-10  $\mu$ l/min), to ensure that the regeneration solution stayed in the system long enough to elute any remaining bound analyte. Regeneration of the chips used in this study was performed 1) after the washing procedure at the end of an analyte injection, and 2) whenever a DNA duplex was formed and the non-biotinylated strand needed to be removed. To verify that the regeneration procedure was successful, the RU signal was monitored after the procedure.

## **2. DNA-Protein Interactions**

### **Biomolecular Interaction Analysis**

All the interaction analyses were performed according to the following procedures. In all binding analyses, the derivitized chips were equilibrated with injections

of running buffer (HBS-EP) prior to any binding analysis. In addition, all oligonucleotides and proteins were equilibrated in the BIAcore running/flow buffer (HBS-EP) to minimize any refractive index differences between the samples and the running/flow buffer.

After the sensor chip surface had been equilibrated, 10  $\mu$ l-50  $\mu$ l aliquots of the protein of interest (*analyte*) were injected over the *ligand*. The binding events were monitored by the biosensor; the signal produced in this procedure as in any other binding event, corresponded to the change in the refractive index of the sensor chip due to the association and dissociation events of the analyte to the immobilized molecule. After the injection of the *analyte*, an automated washing procedure with running buffer (HBS-EP) was performed to remove any bound/unbound analyte. If any *analyte* was still bound, an injection of regeneration solution was performed to remove/elute any *analyte* that did not come off during the washing procedure. Once the *ligand* was freed of any *analyte*, another aliquot of the protein of interest was injected.

#### **a) Formation of DNA Duplexes.**

Immobilization of 5'-GTG TAC GTT AAC GGA TCC CCG GGT ACC GAG C/3BioTEG/-3' (labeled 'normal' strand) created a positive control for binding to SSB and was predicted to be a negative control for UDG since no uracil or abasic lesions are present in the sequence. The normal DNA strand was subsequently hybridized with its 'complementary DNA strand' to form a '**normal**' duplex for further analysis with UDG. In addition, a '**gapped**' duplex was formed by hybridizing the 'upstream' and 'downstream' complements, forming a gap at base 16 of the 'normal' strand. This 'gapped' duplex served as a substrate for Xpol  $\beta$ .

Immobilization of 5'-GTG TAC GT/idSp/ A ACG GAT CCC CGG GTA CCG AGC /3BioTEG/ -3' (labeled 'abasic' strand), created a positive control for binding to SSB and was predicted to be a substrate for UDG due to the presence of the abasic site. The 'abasic' DNA strand was subsequently hybridized with its 'complementary DNA strand' to form an '**abasic' duplex** for further analysis with UDG.

Immobilization of 5'- GTG TAC GTpU AAC GGA TCC CCG GGT ACC GAG C (Biotin-TEG) 3' created a positive control for binding to SSB and was predicted to be a substrate for UDG due to the presence of the pseudo-uracil base. The 'pseudoU' DNA strand was subsequently hybridized with its 'complementary DNA strand' to form a '**pseudoU' duplex** for further analysis with UDG.

#### **b) Single Strand Binding (SSB) Protein.**

SSB was injected over sensor surfaces immobilized with 'normal', 'abasic', and 'pseudoU' immobilized oligonucleotides. The percentage of  $R_{MAX}$  achieved was utilized as an indicator of the presence and integrity of the DNA ligand.

#### **c) Uracil-DNA Glycosylase (UDG).**

UDG was injected over sensor surfaces derivitized with 'normal', 'abasic', and 'pseudoU' single-strand oligonucleotides, as well as the corresponding duplexes.

#### **d) Association of UDG with (SSB + DNA).**

UDG was injected over surface derivitized with 'normal' DNA which had SSB bound to it.

#### **e) DNA Polymerase $\beta$ .**

Xpol  $\beta$  was injected over sensor surfaces containing 'gapped' duplex ligands.

The apparent stoichiometry of the surface complex was calculated using equation 4 as previously described for BSA-warfarin interactions.

## CHAPTER 3

### RESULTS AND DISCUSSION

Although mechanisms of the BER pathway and uracil removal from DNA by UDG have been investigated, monitoring the recognition of uracil by UDG in real-time by SPR has only been done for UDG mutants, and additional protein-protein interactions in BER still need to be addressed. *The goal of this research was to establish protocols for the immobilization of BER substrates of interest as well as binding conditions in order to characterize the interactions among the proteins proposed to be involved in the initial stages of the BER pathway using the biosensor BIAcore X* (Chapter 1, Figure 1). Initially, immobilization of BSA on a CM5 chip (Figure 10) and the binding of phenol red (Figure 11) and warfarin (Figure 12) to BSA were monitored using the biosensor BIAcore X as a model system. With that accomplished, immobilizations of various single-stranded DNA substrates (Figures 13-16) were performed. These immobilized oligonucleotides were later hybridized (Figures 17-20) to selected non-biotinylated complementary oligonucleotides to form duplexes that served as substrates for the proteins under investigation: single strand DNA binding (SSB) protein, uracil-DNA glycosylase (UDG), and *Xiphophorus* DNA polymerase  $\beta$  (*Xpol*  $\beta$ ) (Figures 21-25 and 29).

## *1. General Protocols*

### **Immobilization of a model protein**

In order to understand how the instrument detects binding and to determine optimal immobilization/interaction conditions, we began by producing a CM5 sensor chip containing bovine serum albumin (BSA). Next, we injected at independent times phenol red and warfarin over the immobilized BSA to monitor binding events.

Immobilization of BSA on CM5 sensor chips was easily achieved following procedures stated in Materials and Methods. A single injection of 20  $\mu$ l (1 mg/ml) at a flow rate of 10  $\mu$ l/min produced a response of around 1000 RU's, indicating  $\sim$  1 ng of protein immobilized. Figure 10 shows the typical immobilization response produced after derivatization of a CM5 chip with BSA.

### **Immobilization pH-scouting**

This procedure was performed in order to find the appropriate immobilization pH. In order to increase the attraction between the overall negatively-charged dextran surface of the CM5 sensor chip and the ligand to be immobilized, a lower pH is usually necessary, even though this is not optimal for the coupling chemistry of the immobilization step. BSA was diluted in sodium acetate buffers of different pHs (4.0, 4.5, 5.0, and 5.5) and injected at a final concentration of 30  $\mu$ g/ml, followed by an injection of wash solution (1 M ethanolamine-HCl pH 8.5 or 50 mM NaOH). In our case, the pH-scouting procedure indicated that pH 5.0 was the appropriate immobilization pH. The results obtained from our pH-scouting experiment are summarized in Table 1.

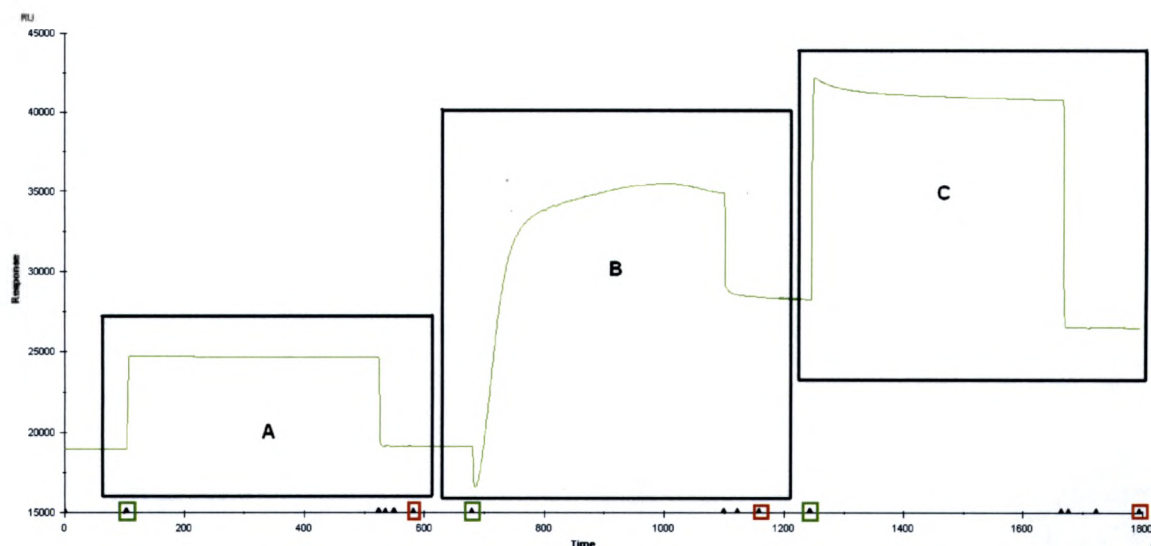


**Figure 10. Successful derivatization of a CM5 sensor chip with BSA.** This immobilization procedure consists of three steps: A) activation of the surface, B) immobilization of protein, and C) capping of surface. After the surface is activated the signal is considered the baseline. After the capping step, the signal observed represents the amount immobilized on the chip. The capping procedure is done to avoid further immobilization of ligand; ethanolamine deactivates (“caps”) the succinimide esters previously activated with the EDC/NHS solution during the activation step. In this sensogram the green squares indicate the beginning of the injection of the corresponding solutions and the red squares indicate the end of the injection. The actual amount immobilized is the RU value obtained after the capping step. In this immobilization, the amount immobilized was ~900RU’s.

**Table 1. Immobilization pH- scouting.** Response units obtained in a pH-scouting exercise. BSA (1mg/ml) was prepared in each buffer to a final concentration of 30 µg/ml. Injections of 20 µl were performed. Buffer at pH 5.0 produced the highest immobilization amount.

Buffer	BSA concentration	response (RU's)
pH 4.0 Sodium Acetate	30 µg/ml	13175.3
pH 4.5 Sodium Acetate	30 µg/ml	19925.5
pH 5.0 Sodium Acetate	30 µg/ml	21513.6
pH 5.5 Sodium Acetate	30 µg/ml	13126.1

### **Interaction of BSA with Phenol Red and Warfarin**

After BSA was successfully immobilized we proceeded to perform binding studies using the compounds phenol red and warfarin. Affinity constants for phenol red and warfarin to Human Serum Albumin (HSA) have been reported (27). The reported affinity constants suggested strong binding of these two molecules, individually, to HSA (27). In our study phenol red and warfarin were analyzed, in separate trials, for association with immobilized BSA. In order to obtain true binding, a reference cell was used each time a binding experiment was performed. A reference cell is simply a control channel not derivatized with any ligand. This control channel corrects for effects from non-specific binding and bulk refractive index changes.

The results from these binding studies indicate binding only of phenol red to BSA (Figure 11). Interestingly, when warfarin was passed over the immobilized BSA, no association was detected by the biosensor (Figure 12). The concentration range of warfarin (150nM – 250  $\mu$ M) used for this binding analysis is within the region of concentrations needed in order to observe interactions of warfarin to BSA since the equilibrium binding constant of warfarin for BSA is on the order of  $10 \times 10^5$  1/M (33). However, the equilibrium binding constant for warfarin is near the lower range of sensitivity on the BIAcore X; consequently, the interaction of warfarin with BSA may be hard to detect unless a very large amount of BSA is immobilized. In our case, we were not able to immobilize BSA in sufficient quantities to detect the interactions of warfarin with BSA.

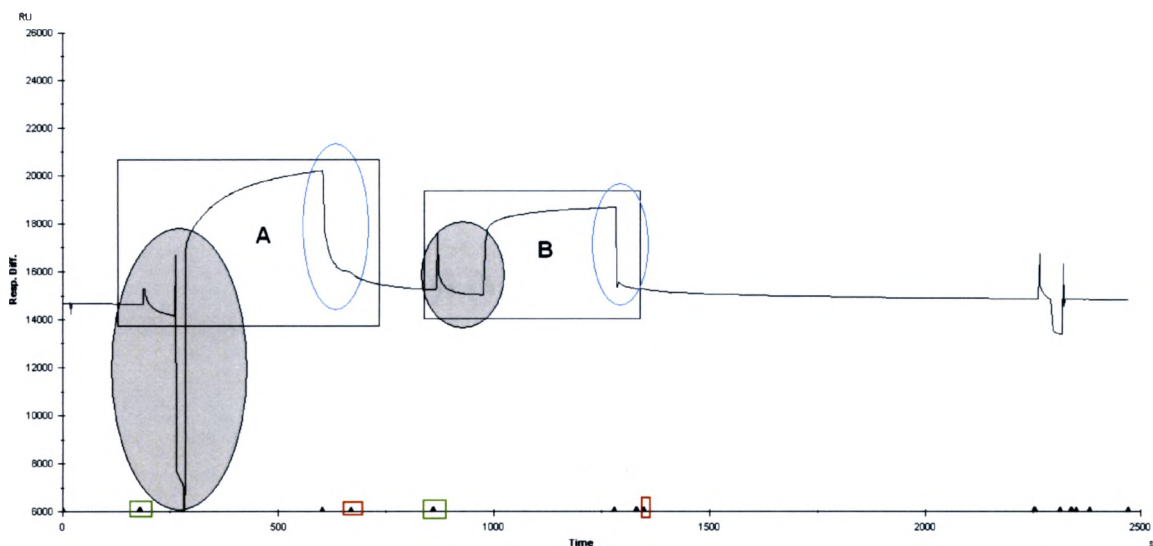


**Figure 11. Association/interaction of phenol red with immobilized BSA.** Regions A and B indicate the two injections of phenol red performed for this analysis. The concentrations of the injections were A)  $2.8 \times 10^{-4}$  M and B)  $2.8 \times 10^{-4}$  M. The green boxes indicate the beginning of the phenol red injections and the red boxes indicate the end of the injections. The areas in grey indicate the presence of air during the injection. From this figure it can be observed that phenol red dissociates quickly from BSA (blue circle), although a very small amount stays bound to the protein.

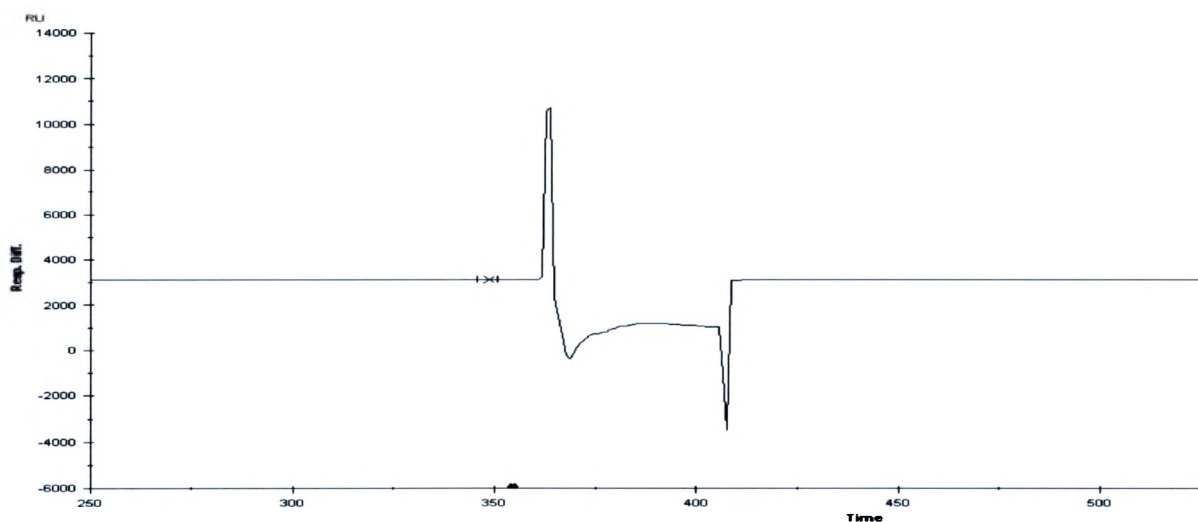


**Figure 12. Warfarin (250uM) injected over immobilized BSA.** The signal produced indicates no binding of warfarin to BSA.

### Immobilization of Biotinylated Oligonucleotides

Once immobilization and interaction conditions were established using BSA as a model system, we proceeded to derivatize streptavidin-dextran matrix chips (SA) with several biotinylated oligonucleotide substrates for UDG. Immobilizations of these biotinylated molecules were easily achieved by following the procedures described in the Material and Methods section. The immobilizations of normal-DNA, abasic DNA, and pseudouracil-containing DNA are presented in Figures 13-16. The purpose of preparing several SA chips with different forms of biotinylated DNA, including duplexes, was to observe the activity of the proteins with the different substrate forms (single- and double-stranded DNA).

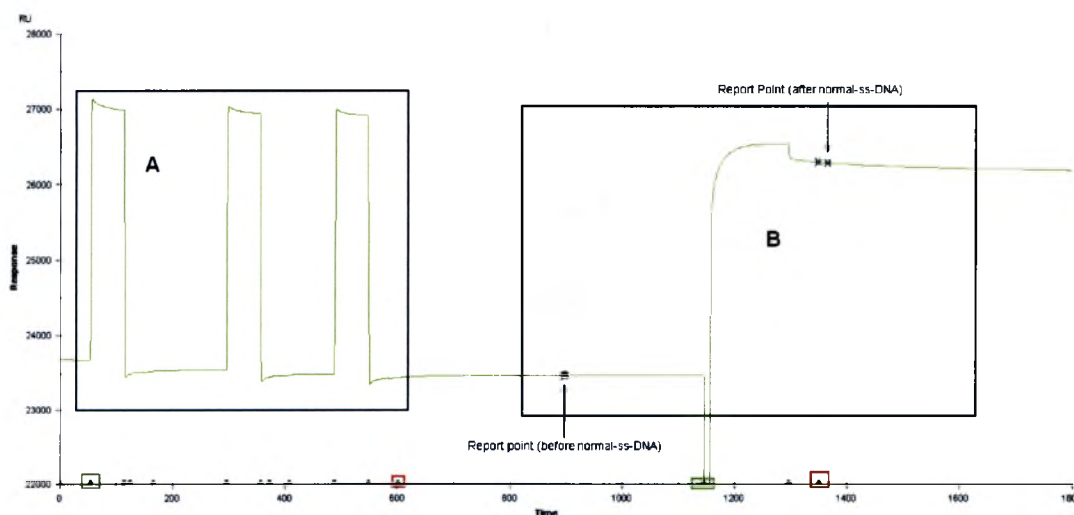


**Figure 13. Immobilization of a biotinylated oligonucleotide (normal-ssDNA).** The two main steps include A) surface cleaning with NaOH/NaCl and B) immobilization of a biotinylated oligonucleotide on a SA sensor chip. This two-step immobilization procedure was used for all of the subsequent immobilizations of biotinylated oligonucleotides. In order to determine the response units for the immobilization of the substrate, report points were utilized they were set before and after the injections. The response produced by the immobilization of the biotinylated DNA in this case was 2800RU's, indicating that approximately 3 ng of DNA were immobilized.

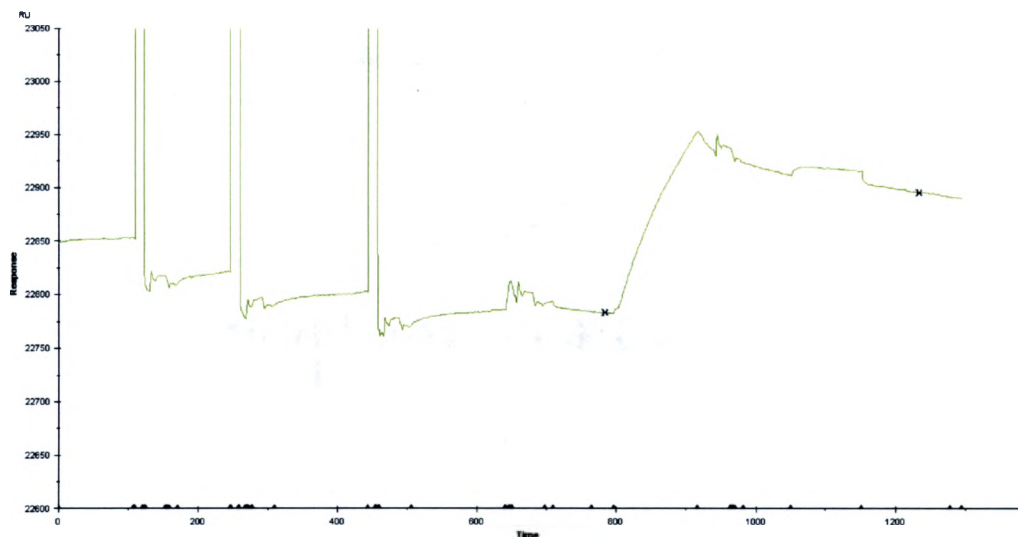


**Figure 14. Immobilization of a smaller amount of normal-ssDNA on a SA chip.** In this case the response produced was 120 RU, indicating approximately 0.1 ng of DNA was immobilized.

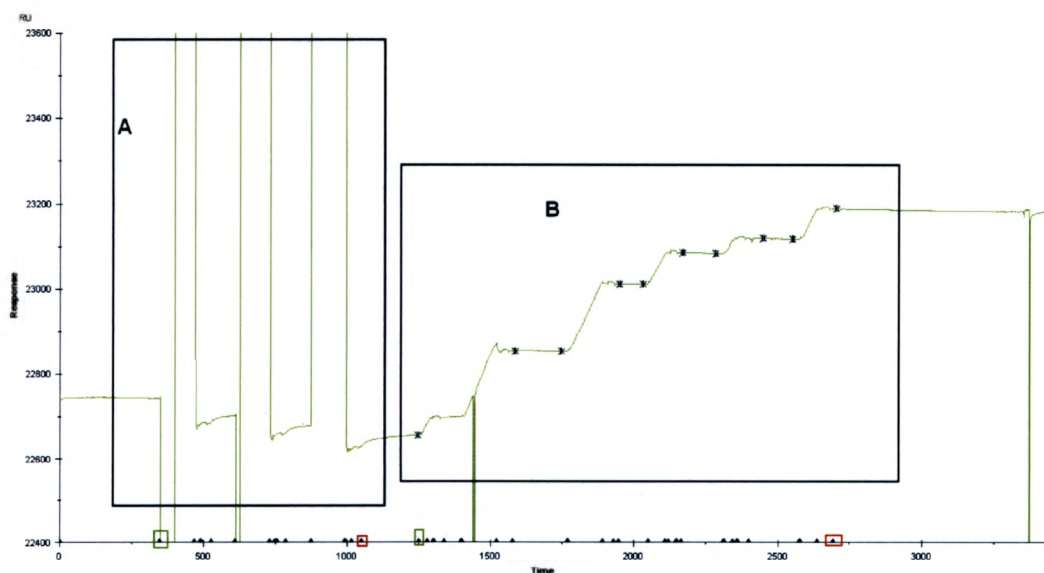


**Figure 15. Derivatization of a SA chip with abasic-ssDNA.** In this immobilization procedure, a response of 532 RU's was produced; indicating approximately 0.5 ng of DNA was immobilized. Small injection volumes were performed to achieve the desired response. Section A indicates preparation of the binding surface and section B indicates the immobilization injections. The green square in section A indicates the beginning of the activating solution injections and the red square indicates the end of injections. In section B, the green square indicates the beginning of oligonucleotide injections and the red square indicates the end of the oligonucleotide injections. A total of five oligonucleotide injections were performed to reach the desired immobilization response.

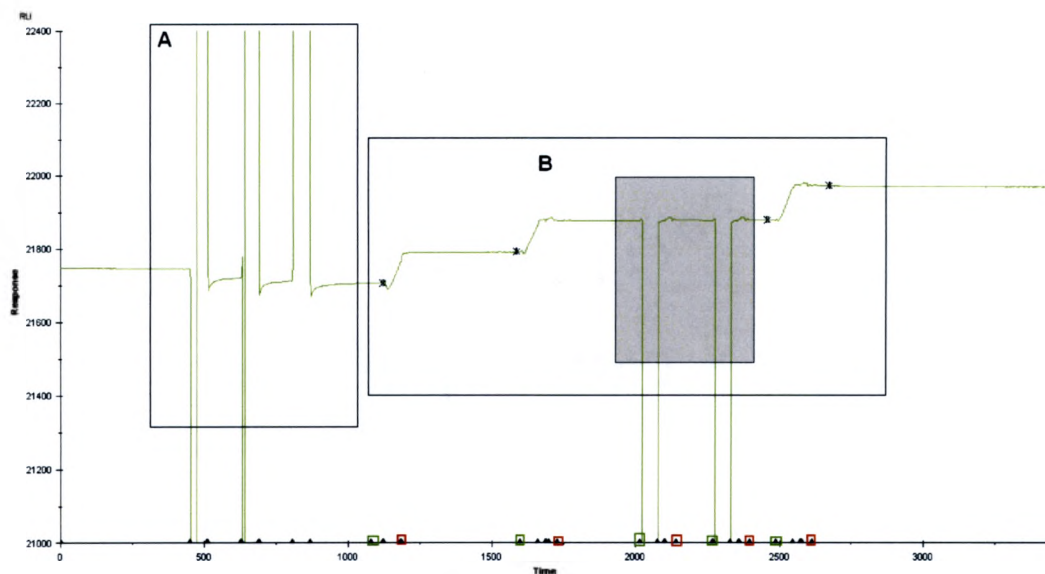


**Figure 16. Immobilization of pseudouridine containing ssDNA on a SA chip.** Three injections of activating solution were performed (A) to prepare the surface for derivatization. The desired immobilization response was achieved by performing five small volume injections of pseudouridine containing ssDNA (B); the green squares indicate the beginning of the ligand injections and the red squares indicate the end of the injections. The immobilization response obtained was 260 RU.

## 2. Biomolecular Interactions

### Formation of Normal and “Gapped” DNA Duplexes *in situ*

Gap-containing DNA duplexes were also produced with the purpose of observing binding events of  $X_{\text{pol}} \beta$  to these duplexes. The “gapped” duplexes were formed by hybridizing two short oligonucleotides, referred to as upstream and downstream DNA strands, to the immobilized oligonucleotide. The final product was double stranded-DNA containing a gap at base pair 16 (Figure 17).

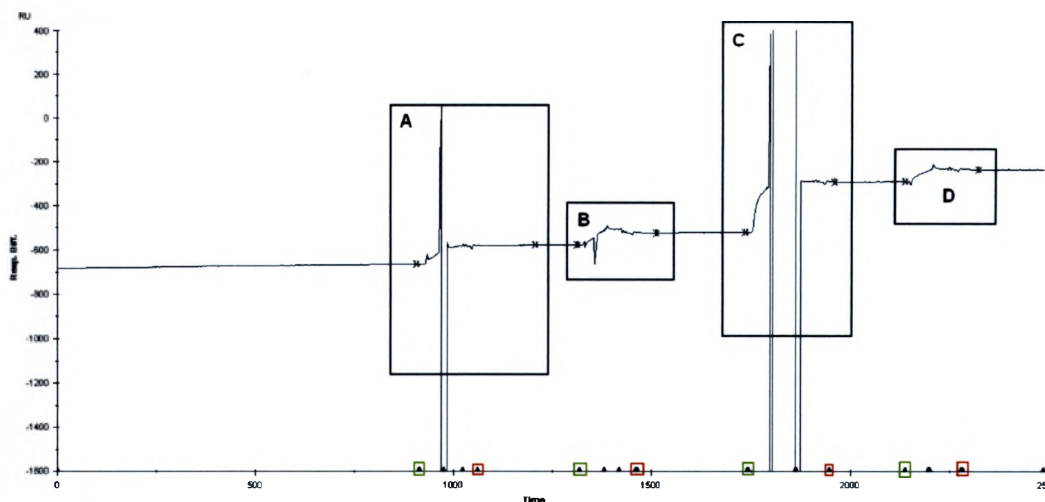


**Figure 17. Formation of a gapped duplex DNA (A-D).** The duplex was formed by injecting the upstream and downstream DNA strands onto the normal-DNA. The hybridization produced a response of 425 RU's. Areas A, B, and D indicate the injections of the upstream DNA strand and area C is the injection of the downstream DNA strand. In section D, it can be observed that saturation levels were reached since the increase in response is very small. The response obtained from the immobilization of the normal-DNA strand was ~500RU's therefore based on the amount immobilized the maximum response expected would be ~ 500RUs.

Besides this gapped double stranded DNA, other forms of double-stranded DNA were used for association studies of UDG, SSB, and Xpol  $\beta$ . Figures 18-20 show the response produced by hybridization of complementary oligonucleotide to produce duplex DNA on the SA chips. Since the stoichiometry of binding between each oligonucleotide is 1:1 in order to produce duplex DNA, it is easy to predict the maximum response in RU's that would be expected for the formation of 100% duplex DNA on the SA chip. In cases where the hybridization exhibited less than maximal response (Figure 18), the chip was judged to be degraded or no longer useful for binding studies.

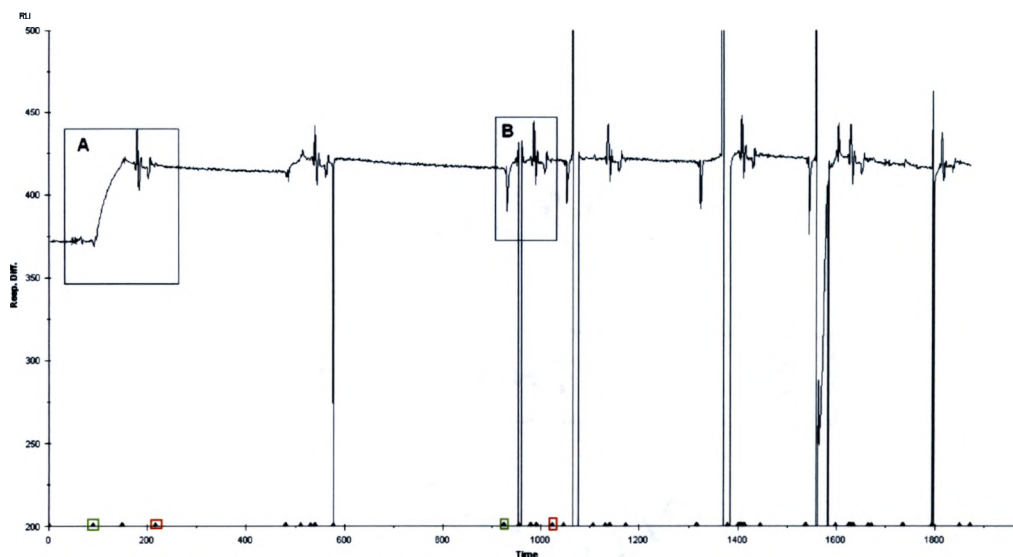


**Figure 18. Hybridization of complementary DNA to form a normal-DNA duplex.**

The hybridization response produced after the final injection of complementary DNA over the biotinylated oligonucleotide was 31RU's. The association response is very low indicating that the immobilized surface was not saturated with the complementary DNA. These results suggested the degradation or instability of the chip since the response only increased 30 RU's after five injections of complementary DNA. The first injection added most of the DNA hybridized (A) and after the third injection the response seemed to reach saturation levels (B). The amount of ligand immobilized produced a response of ~112RU's therefore based on this amount immobilized; the maximum response expected from the hybridization of complementary DNA is ~105RU's.

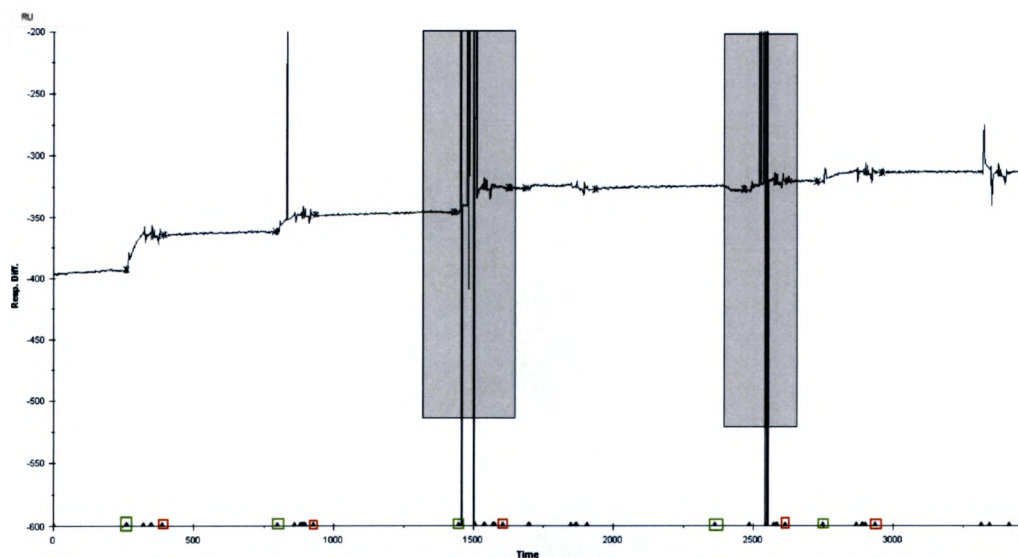


**Figure 19. Successful hybridization of complement DNA to form a normal-DNA duplex.**

After five injections of complement DNA the immobilization response was 80 RU's. The response for the immobilization of normal-DNA was 112 RU's therefore the  $R_{max}$  expected is ~105RUs.

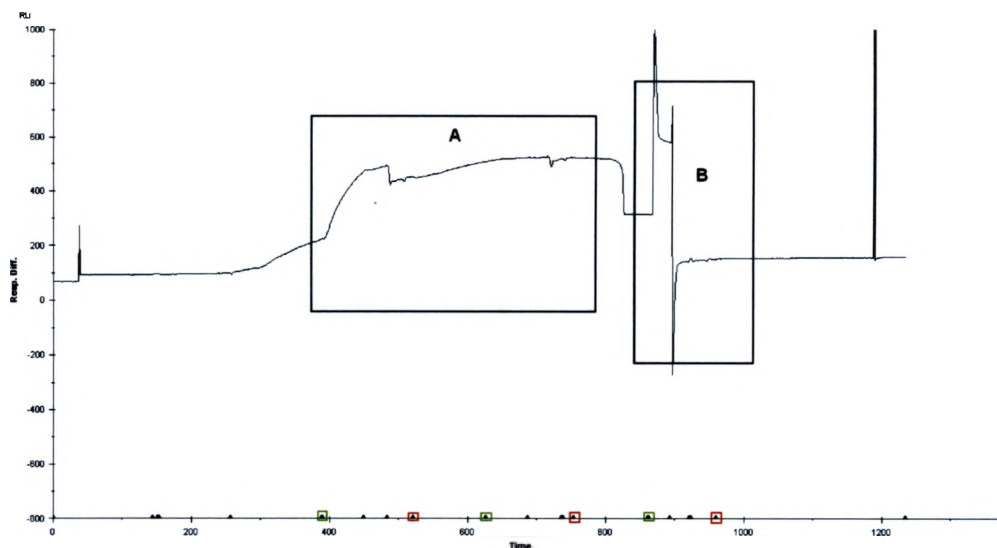


**Figure 20. Formation of an abasic duplex DNA (A) and regeneration of the chip's surface (B).** The regeneration procedure did not free completely the analyte (complement) from the immobilized ligand. Two injections of the complement DNA (A) were required to reach hybridization saturation levels; the maximum response expected was ~500RU's. The hybridization response for the formation of the duplex DNA was 200 RU's. The signal after regeneration was 30 RU's indicating the presence of remaining complement bound to abasic DNA.

### DNA-Protein Interactions

Once the chips were derivatized successfully and the maximum amount of duplex was formed in each case, we performed binding studies using the proteins Single Strand Binding (SSB) protein, Uracil-DNA-Glycosylase (UDG), and *Xiphophorus* polymerase- $\beta$  (*Xpol*  $\beta$ ) to monitor protein-DNA interactions. Protein solutions were injected over the immobilized oligonucleotides and duplexes.

Figures 21, 22, and 24 show sensorgrams of SSB binding to oligonucleotide substrates. SSB bound very effectively to single strand oligonucleotides, exhibiting the maximum possible response (Figures 21, 22), and was therefore used as an indicator of the actual presence of DNA on the chip. The binding between SSB and single strand oligonucleotide substrates is so strong that several regeneration procedures were always

needed to remove all of the bound SSB. Binding of SSB to duplex DNA-immobilized SA chips was not evident and diminished binding of SSB is observed when single-stranded DNA capable of forming a quadruplex structure is used (Karl Jasheway, Wendi David, unpublished results). Chips derivatized with pseudouridine containing oligonucleotide were typically unstable and we were unable to demonstrate effective binding by SSB (Figure 24).

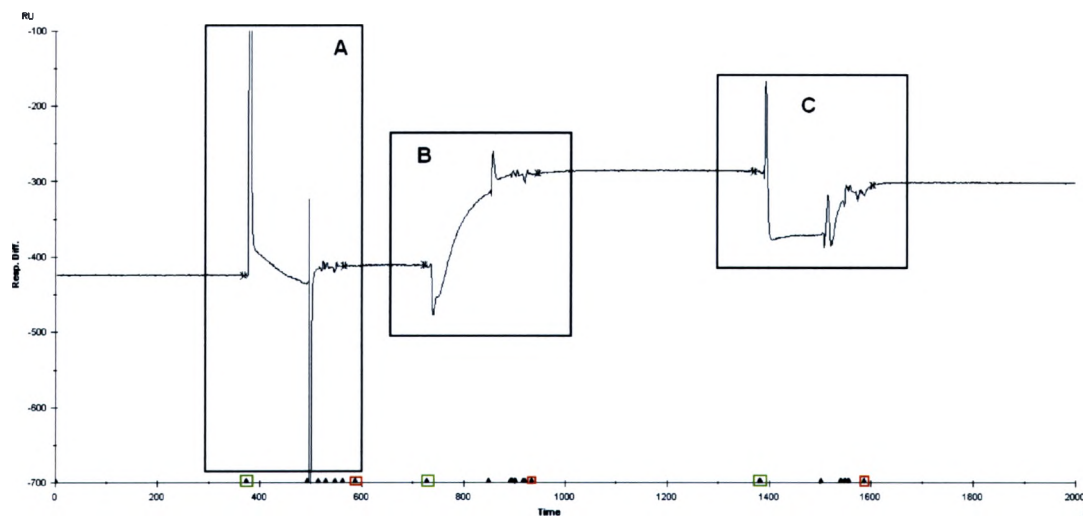


**Figure 21. Binding of SSB protein to single strand normal-DNA.** A) The sensor surface was regenerated with glycine solution before binding studies and C) after binding studies with 0.1% SDS. The green squares indicate the beginning of injections and the red squares indicate the end of injections. B) Binding of SSB protein to ligand produced a response of about 120 RU's. After the surface was regenerated once with 0.1% SDS we observed that the signal only dropped to about 20 RU's, indicating the very strong binding between SSB and single-strand DNA.

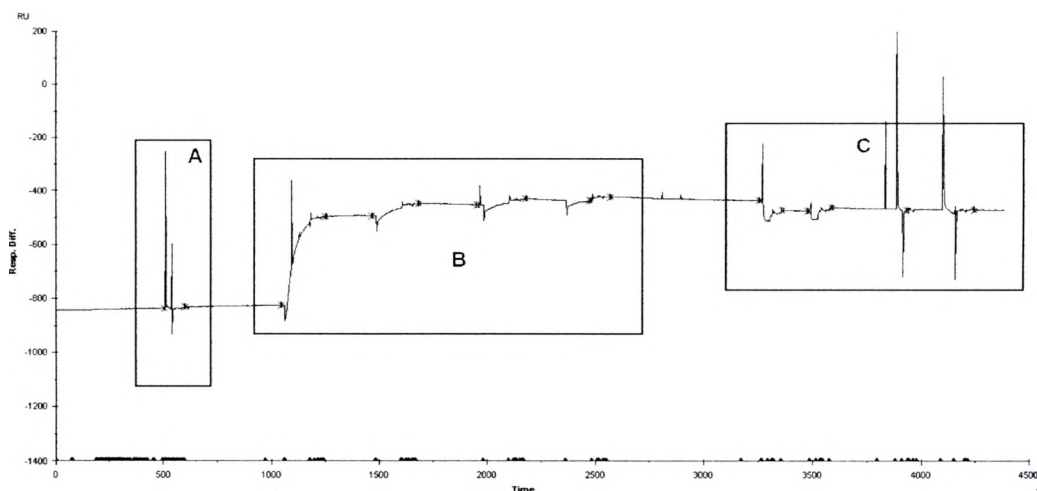


**Figure 22. Additional binding of SSB to single-strand normal-DNA.** A) Regeneration of binding surface with 0.1% SDS, B) Binding of SSB to normal-DNA, and C) Regeneration with two injections of 0.1% SDS followed by two injections of Glycine (pH 2.5). After the first regeneration procedure no change in the base line was observed indicating that the chip was free of bound analyte. Four small volume injections of SSB protein were injected until saturation levels were reached at a response of 400 RU's. The binding surface was regenerated with short injections of 0.1 % SDS. However, the signal only dropped 50 RU's indicating that a large amount of SSB protein was still bound to the ligand.

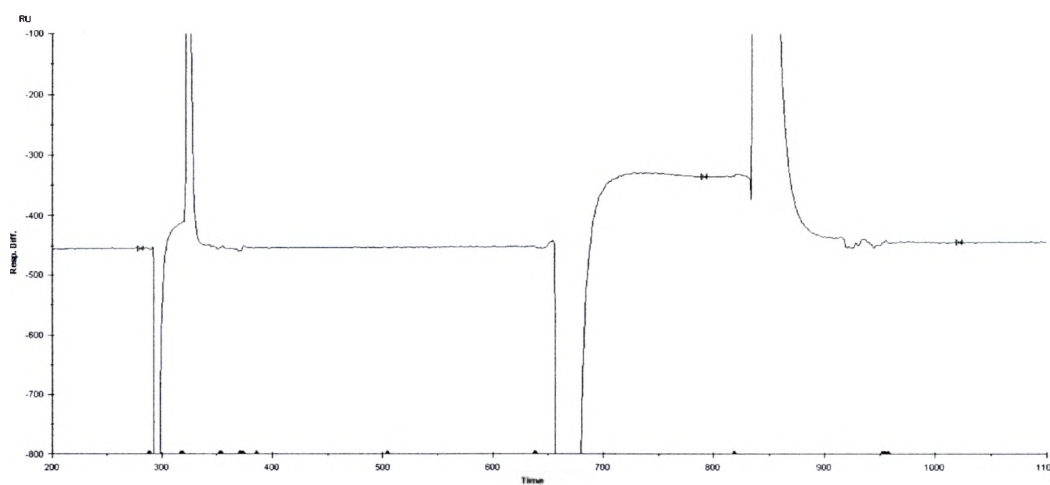


**Figure 23. Binding of UDG to pseudouridine containing ssDNA.** Samples injected were dilutions from the stock solution of 1/10 and 1/6. An equilibrium binding of 120RU's was observed for the second injection (1/6).

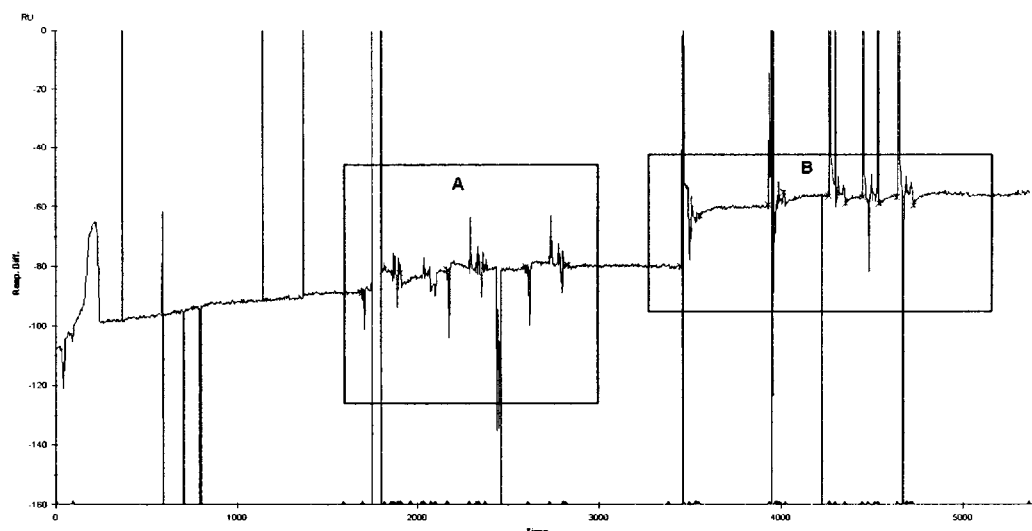


**Figure 24. Protein-DNA interaction followed by surface regeneration.** SSB protein interacting with immobilized pseudouridine containing ssDNA. (A), followed by regeneration of surface with 0.1% SDS and Glycine pH 2.5 (B). During this procedure it was observed that analyte (SSB) hardly bound to the ligand producing a response of around 9 RU's (A). After regeneration using 0.1% SDS to remove any SSB bound to the ligand, glycine (pH 2.5) was used to remove any other molecules that did not come off with the 0.1% SDS solution (B). Interestingly, we observed that the signal increased during regeneration, suggesting either the possible association of some of the molecules from the regenerating solutions to the immobilized DNA or removal of some substance from the control surface.

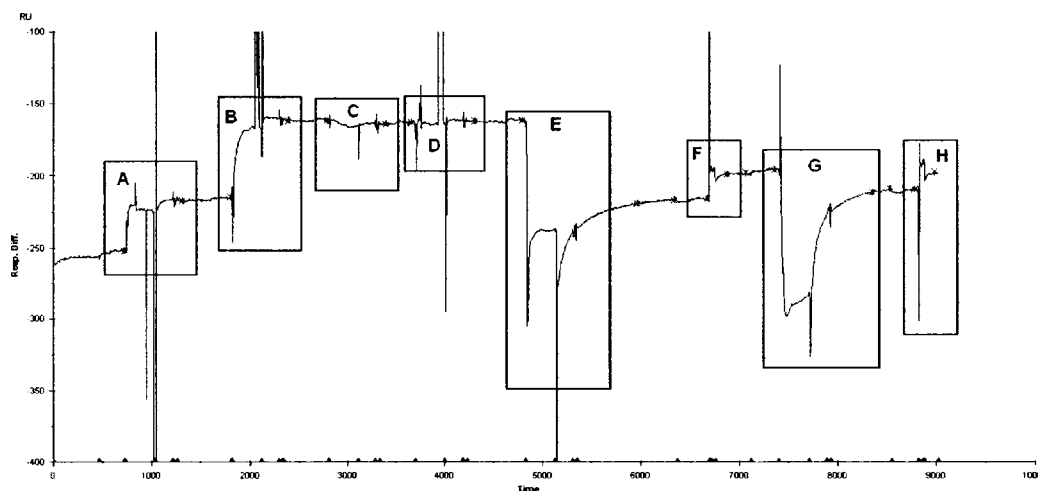


**Figure 25. Formation of a gapped duplex DNA and binding by Xpol  $\beta$ .** Four injections of A) downstream DNA strand, B) upstream DNA strand, C) downstream DNA strand, and D) upstream DNA strand until the maximum duplex was formed. After duplex formation, Xpol  $\beta$  was passed over the duplex (E) followed by an injection of NaCl (F) another injection of Xpol- $\beta$  (G) and finally an injection of NaCl (H).

From figure 25 it can be observed that formation of duplex DNA was successful (maximum response of 90 RUs was reached) however the injections of *X*pol  $\beta$  (Figure 25, E and G) produced interesting results. It seems as if the protein displaced the hybridized DNA strands (upstream and downstream) since the response dropped. In addition, an unexpected increase in signal during regeneration of the chip may indicate binding of residual analyte in the presence of higher salt (Figure 25, F and H).

### **DNA-Protein-Protein Interactions**

Although the binding studies of SSB were successful, results with UDG and *X*pol  $\beta$  were unexpectedly difficult to obtain and reproduce. Interestingly, our studies indicated that UDG did not show binding to any form of DNA (single-strand or duplex), even when a binary complex of DNA-SSB was formed (Figure 26). In a study by Handa, *et al* it was found that *E. coli* UDG did not bind to DNA unless SSB was first bound to DNA forming a DNA-SSB binary complex, in which case binding of UDG to DNA was observed (13). In our study, no binding was observed between UDG and a preformed DNA-SSB complex (Figure 26). This result suggests that our UDG sample was not present in sufficient concentration for a signal to be observed.

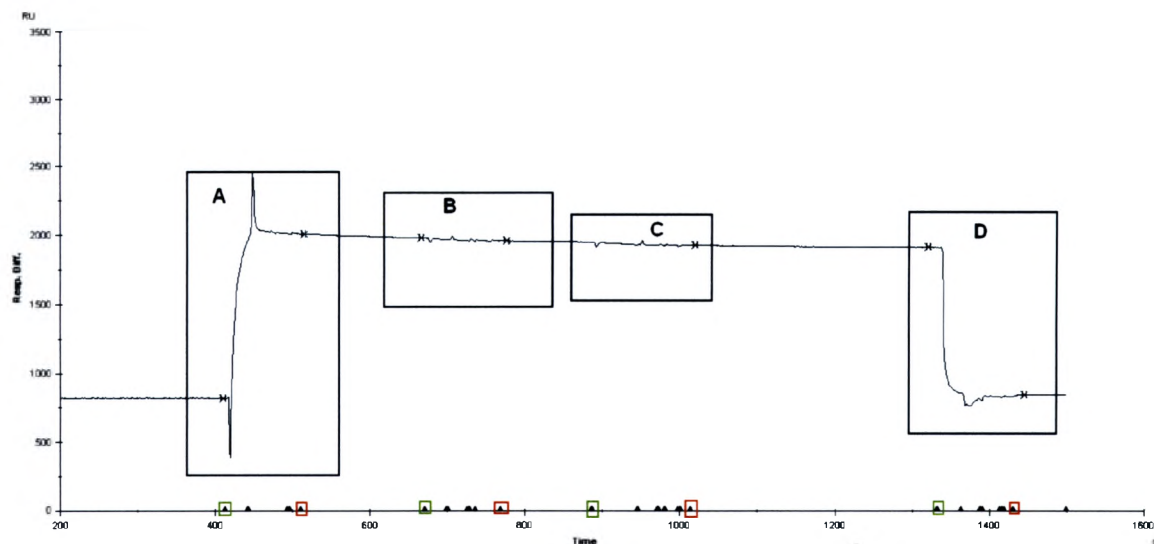


**Figure 26. Interaction of UDG with binary complex (SSB-DNA).** (A) Formation of SSB-DNA complex, followed by two injections of UDG (B, C), and the regeneration of the sensor surface with 0.1% SDS solution (D). From the response obtained, binding of SSB to immobilized DNA can be observed (A) (maximal response obtained from this association at approximately 1200 RUs). When UDG was injected (B and C) the signal drops slightly. (D) The regeneration with 0.1% SDS did not completely remove SSB from the immobilized oligonucleotide.

Due to the results obtained from UDG and *X*pol  $\beta$  we believed that the proteins may have been degraded and/or were no longer active. In order to verify the presence and purity of UDG and *X*pol  $\beta$ , both proteins were analyzed by SDS-PAGE (Figures 27 and 28). The protein *X*pol  $\beta$  was expected to be observed at 39kDa and UDG was expected to be observed at 25kDa. Surprisingly, the gel revealed no evidence of both proteins. The band observed in lane 2 indicates the presence of an unknown protein in the storage buffer for the protein *X*pol  $\beta$ .

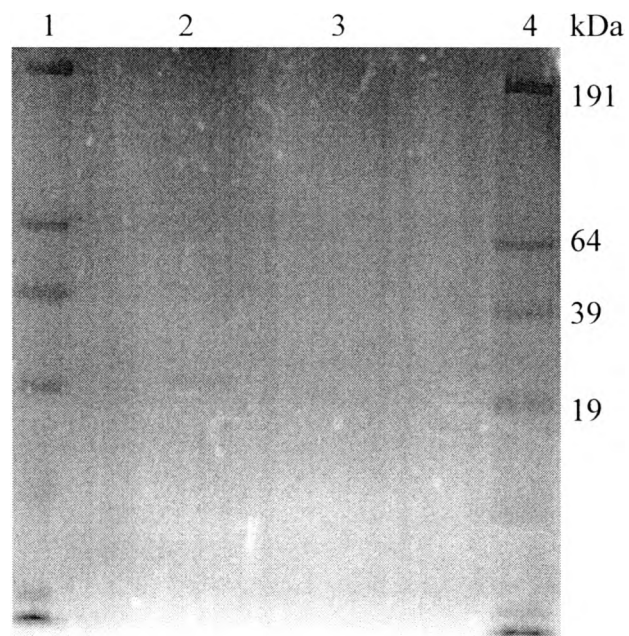


**Figure 27. SDS-PAGE analysis of Xpol  $\beta$  and UDG.** Lanes 1 and 4 correspond to the protein ladder (SeeBlue® Pre-Stained Standard) containing molecular weights standards, lane 2 corresponds to Xpol  $\beta$ , and lane 3 corresponds to UDG. The procedure was performed to verify that the proteins were present in their stock solution.

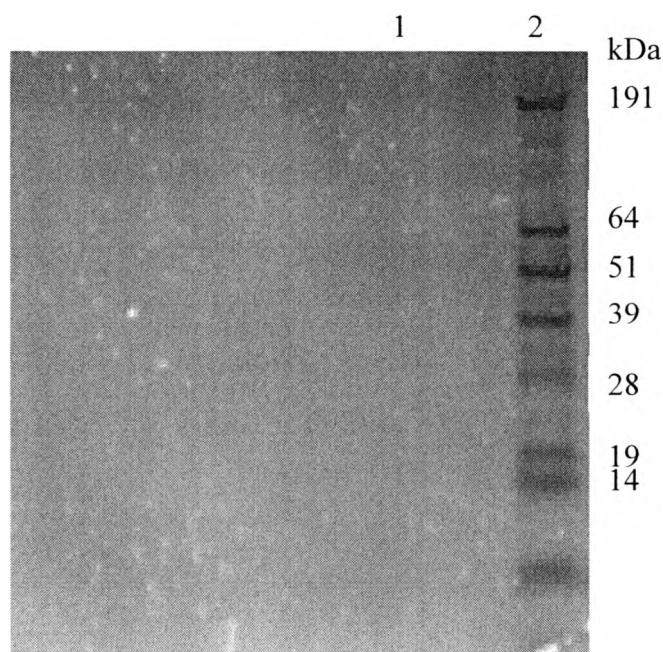


**Figure 28. SDS-PAGE analysis of UDG.** Lane 1 corresponds to UDG and lane 2 corresponds to the protein ladder containing molecular weights standards. The procedure was performed to verify that UDG was present in the stock solution.

These results suggested absence or inactivity of both enzymes UDG and *X*pol  $\beta$  in their buffer solutions. In the case of *X*pol  $\beta$ , it is possible that the enzyme is present in sufficient amount. In order to minimize any aberrant sensogram effects from the *X*pol  $\beta$  storage buffer, we tried buffer exchange of *X*pol  $\beta$  from the storage solution into HBS-EP running buffer. After several purification procedures we repeated the binding studies with the “purified” *X*pol  $\beta$  but the results were still the same (data not shown).

### ***3. Regeneration and Stability Protocols***

After sensor surfaces were derivatized with the desired biotinylated oligonucleotide (ligand) and binding studies were carried out with the protein or oligonucleotide (analyte) of interest, the sensor surfaces were regenerated with different regeneration solutions (0.1% SDS (protein), glycine pH 2.5 (protein), or 1 M NaCl (DNA)) depending on what analyte was bound to the ligand. The purpose of this procedure was to free the ligand of bound analyte so that the chip could be used multiple times without modifying the immobilized ligand and analysis could be reproduced for verification purposes. A representative sensogram is shown in figure 29: after regeneration of a normal-DNA/SSB complex, a **normal duplex** was formed.

In some cases, however, the regeneration solution not only removed the bound analyte but also some of the ligand and as a consequence ligand was lost and the response signal (base line) dropped. One way to correct this is simply to add more of the ligand solution by repeating the immobilization procedures. As long as each oligonucleotide-immobilized chip could form the maximum amount of duplex when exposed to the correct complement, the chip was considered to be reusable.

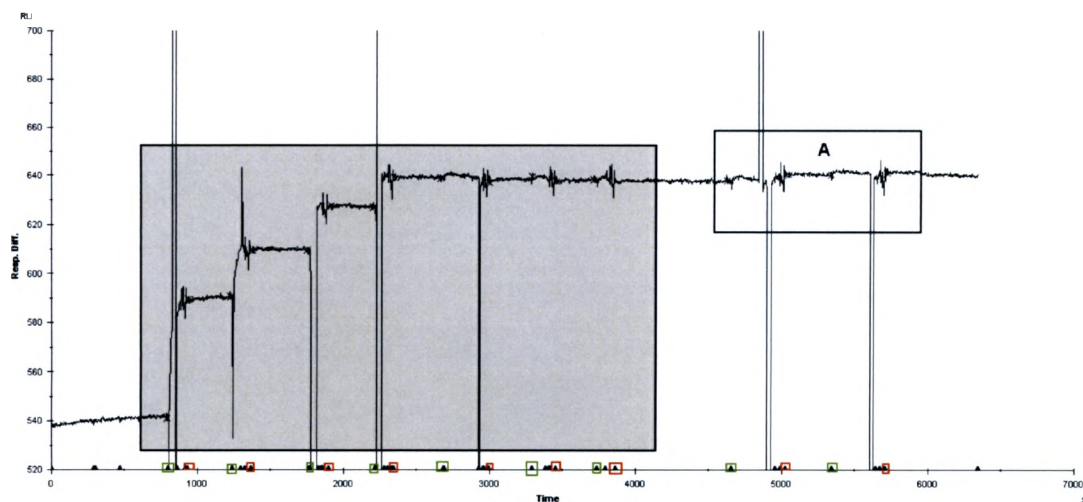


**Figure 29. Protein-Protein-DNA interaction.** Hybridization of the upstream and downstream DNA strands (analyte) to immobilized normal-DNA (gray area) immediately after surface was exposed to SSB and UDG. The purpose of this procedure was to test the stability of the chip by reforming a DNA duplex. A saturation level response was reached (100 RUs), indicating the stability of the chip. The last two injections (A) are buffer injections (1 M NaCl) that were performed to free the ligand from complementary up- and downstream DNA strands.

Throughout our studies, chips derivatized with ‘abasic’ and ‘pseudouridine’ oligonucleotides were not as stable as they should have been. Typically after regeneration the chips would start to degrade at a very fast rate compared to 5’-biotinylated oligonucleotides immobilized for other studies in the David lab. The most binding analyses that we were able to perform on these ‘abasic’ and ‘pseudoU’ chips were three. In addition it was not possible to effectively re-derivatize these chips as for other SA chips immobilized with oligonucleotides. In other studies in our lab chips were regenerated multiple times and binding analyses performed were reproduced multiple times; therefore 5’-biotinylated, unmodified oligonucleotides are recommended for the most effective immobilizations of DNA.

In order to verify the stability and quality of chips containing duplex DNA (formed from hybridization of an oligonucleotide complementary in sequence to the immobilized single-stranded oligonucleotide, *or* from an immobilized oligonucleotide hairpin capable of forming a small duplex region) binding studies of the intercalator ethidium bromide were performed. Ethidium solutions (450 nM – 18  $\mu$ M, in normal HBS-EP buffer) were allowed to interact with a hairpin duplex at 30  $\mu$ L per minute for 4 minutes. An extremely fast on and off rate was observed, precluding accurate determination of  $k_{\text{on}}$  and  $k_{\text{off}}$  (Figure 30). However, a steady-state equilibrium of binding was achieved rapidly at all concentrations and a plot of response in the steady-state region (RU) *versus* concentration (M) yielded an equilibrium binding constant of  $4.2 \times 10^5 \text{ M}^{-1}$ , in agreement with published binding constants for ethidium bromide/duplex DNA interactions determined by SPR (Figure 31) (34).

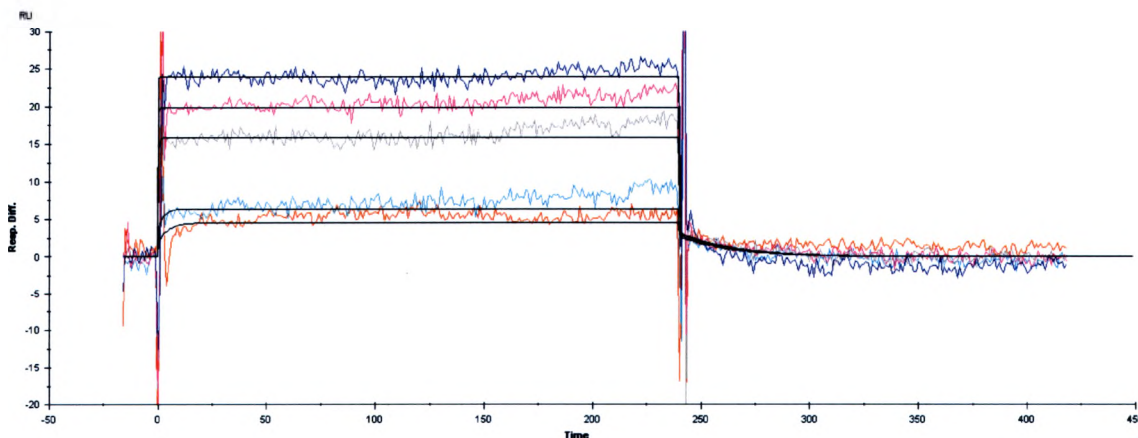


**Figure 30.** Interaction of Ethidium with a hairpin oligonucleotide.

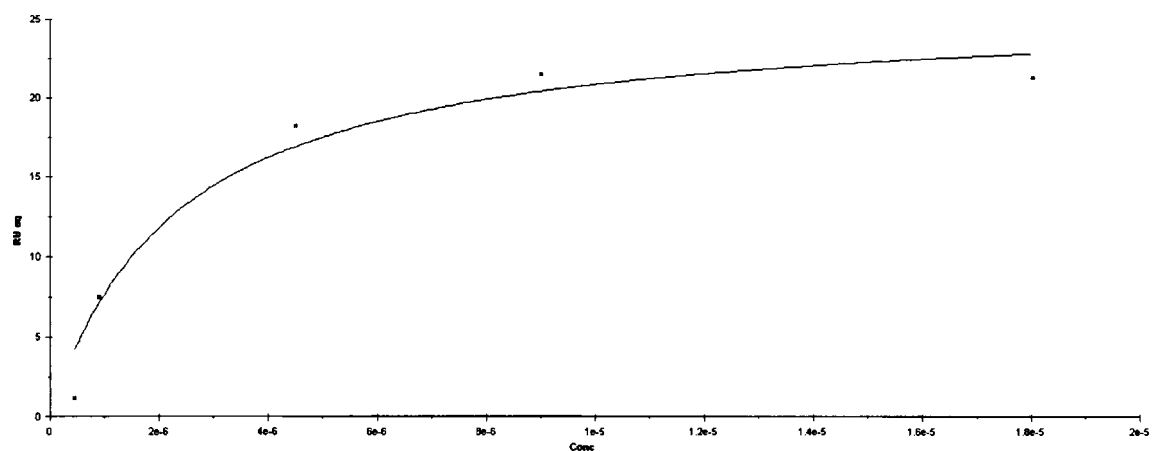


**Figure 31. Determination of  $K_D$  for ethidium/duplex DNA interaction.** Relative response for Ethidium intercalation was plotted *versus* Ethidium concentration to yield an equilibrium binding constant for the interaction.

### *Summary*

Bovine serum albumin (BSA) was immobilized on a CM5 chip and binding studies with phenol red and warfarin were performed. These initial studies were used to gain experience with immobilization protocols and binding conditions and were later followed by the immobilization of various DNA substrates and binding studies with the proteins uracil-DNA glycosylase (UDG), single strand DNA binding protein (SSB), and *Xiphophorus* recombinant DNA polymerase- $\beta$  ( $Xpol \beta$ ). The immobilizations of BSA were successfully achieved and reproducible. However, the results obtained from the binding studies of phenol red and warfarin to BSA showed binding only of phenol red. Nonetheless the results obtained for the binding of warfarin to BSA are reasonable since the affinity constant of warfarin for BSA is in the lower limits of the detection range of the BIAcore X and the amount of BSA immobilized was insufficient for appreciable warfarin binding to be observed.

After initial experiments with BSA, various single stranded oligonucleotides were immobilized on streptavidin (SA) coated sensor chips: 'normal'-DNA, 'abasic' DNA, and 'pseudouracil' containing DNA. The substrates were either single- or double-stranded DNA. In order to observe activity of the proteins, normal-duplex DNA or gapped-duplex DNA were produced.

The immobilized substrates were exposed to the proteins under investigation by carrying out binding studies. During the binding studies, it was observed that SSB was the only protein that would interact with its respective substrate. The sensograms produced by the binding analyses of the proteins UDG and  $Xpol \beta$  were inconclusive.

In each case this behavior was believed to be caused by protein degradation or insufficient amount of protein.

In order to verify if the proteins were present in their stock solution, SDS-PAGE analysis was performed. No UDG was detected and a second SDS-PAGE analysis showed no evidence of UDG. It could be that the concentration of UDG was very low or the protein was not longer active which explains why no association was observed during the binding studies. *Xpol*  $\beta$  also appears to have degraded during storage.

Sensor chips that were derivitized and used in binding studies were regenerated with the appropriate regeneration solution. This procedure was performed in order to free the ligand of any bound analyte with the purpose of reusing the chip for more studies. However, chips derivitized with 'abasic' and 'pseudouracil' oligonucleotides appeared to degrade at a very fast rate by this procedure. Chips derivitized with normal single-stranded oligonucleotides were much more stable and available for multiple applications. The formation of duplex DNA from a single-stranded hairpin oligonucleotide was verified by intercalation of ethidium bromide. An equilibrium binding constant of  $4.2 \times 10^5 \text{ M}^{-1}$  was obtained for the interaction, in excellent agreement with literature (34).

Future studies will continue to establish immobilization protocols for the DNA substrates as well as determine binding conditions for the proteins used in this study. Also binding studies between the different proteins involved in the BER pathway may be more successful by immobilizing the proteins (UDG, for instance, instead of an oligonucleotide substrate) on to the sensor surface. Additionally, regeneration protocols need to be established in order to avoid degradation of the sensor chips

## REFERENCES

1. Krokan, H. E.; Standal, R.; Slupphaug, G. *Biochem. J.* **1997**, 325, 1-16.
2. Schärer, O. D. *Angew Chem. Int. Ed.*, **2003**, 42, 2946-2974.
3. Beard, W.; Wilson, S. *Mutat. Res.* **2000**, 460, 231-244.
4. Wilson, S. *Mutat. Res.* **1998**, 407, 203-215.
5. Pingfan, L.; Burdzy, A.; Sowers, L. *Chem. Res. Toxicol.* **2000**, 15, 1001-1009.
6. Wood, R. D. *Annu. Rev. Biochem.* **1996**, 65, 135-167.
7. Hang, B.; Singer, B. *Chem. Res. Toxicol.* **2003**, 16, 1181-1190.
8. Nilsen, H.; Krokan, H. E. *Carcinogenesis.* **2001**, 22, 987-998.
9. Kumar, V.; Varshney, U. *Nucl. Acid Res.* **1994**, 22, 3737-3741.
10. Panayotou, G.; Pearl, L. H. *BIAjournals.* **2001**, 1.
11. Kumar, N. V.; Varshney, U. *Nucl. Acid Res* **1997**, 25, 2336-2343.
12. Mol, C. D.; Parikh, S. S.; Putnam, C. D.; Lo, T. P.; Tainer, J. A. *Annu. Rev. Biophys. Biomol. Struct.* **1999**, 28, 101-128.
13. Handa, P.; Acharya, N.; Vashney, U. *J. Biol. Chem.* **2001**, 276, 16992-16997.
14. Purnapatre, K.; Handa, P.; Venkatesh, J.; Varshney, U. *Nucl. Acid Res.* **1999**, 27, 3487-3492.
15. Tsoi, P.Y.; Yang, M. *J. Biochem.* **2002**, 361, 317-325.
16. Panayotou, G., Brown, T.; Barlow, T.; Pearl, L. H.; Savva R. *J. Biol. Chem.* **1998**, 273, 45-50.
17. Roberts, R. J.; Cheng, X. *Annu. Rev. Biochem.* **1998**, 67, 181-198.

18. Bennett, S. E.; Shimerlik, M. I.; Mosbaugh, D. W. *J. Biol. Chem.* **1993**, 268, 26879-26885.
19. Slupphaug, G.; Mol, C. D.; Kavli, B.; Arvai, A. S.; Krokan, H. E.; Tainer, J. A. *Nature.* **1996**, 384, 87-92.
20. Curth, U.; Genschel, J.; Urbanke, C.; Greipel, J. *Nucl. Acids Res.* **1996**, 24, 2706-2711.
21. Raghunathan, S; Kozlov, A. G.; Lohman, T. M.; Waksman, G. *Nat. Struct Biol.* **2000**, 7, 648-652.
22. Rajendran, S.; Jezewska, M.; Bujalowski, W. *J. Mol. Bio.* **2001**, 308, 477-500.
23. Oehlers, L. P.; Heater, S. J.; Rains, D.; Wells, M. C.; David, W. M.; Walter, R. B. *Comp. Biochem. Phys., Part C*, **2004**, 138, 311-324.
24. Gambari, R.; Feriotto, G.; Rutigliano, C.; Bianchi, N.; Mischianti, C. *J. Phamacol. Exp. Therapeut.* **2000**, 294, 370-377.
25. Torrieri, P.; Ceccarini, M.; Macioce, P.; Petrucci, T. *Anna Ist Super Sanità.* **2005**, 41, 437- 441.
26. Bondeson, K.; Frostell-Karlsson, A.; Fägerstam, L.; Magnusson, Göran. *Anal. Biochem.* **1993**, 214, 245-251.
27. Ulrich, K-H. *Biochem. J.* **1985**, 225, 629-638.
28. Parikh, S. S.; Walcher, G.; Jones, G. D.; Slupphaug, G.; Krokan, H. E.; Blackburn, G. M.; Tainer, J. A. *Proc. Nat. Acad Sci. U S. A.* **2000**, 97, 5083-5088.
29. Fisher, R. J.; Fivash, M.; Casa-Finet, J.; Erickson, J.; Kondoh, A.; Bladen, S.; Fisher, C.; Watson, D.; Papas, T. *Prot. Sci.* **1994**, 3, 257-266.
30. Gotoh, M.; Hasegawa, Y.; Shinohara, Y.; Shimizu, M.; Tosu, M. *DNA Res.* **1995**, 2, 285- 293.
31. Katsamba, P. S.; Navratilova, I.; Calderon-Cacia, M.; Fan, L.; Thornton, K.; Zhu, M.; Vanden Bos, T.; Forte, C.; Friend, D.; Laird-Offringa, I.; Tavare, G.; Whatley, J.; Shi, E.; Widow, A.; Lindquist, K. C.; Klakamp, S.; Drake, A.; Bohmann, D.; Roell, M.; Rose, L.; Dorocke, J.; Roth, B.; Luginbühl, B.; Myszka, D. *Anal. Biochem.* **2006**, 352, 208-221.
32. Izrailev, S.; Stepaniants, S.; Balsera, M.; Oono, Y.; Schulten, K. *Biophys. J.* **1997**, 72, 1568-1581.

33. Yamasaki, K.; Maruyama, T.; Kragh-Hansen, U.; Otagiri, M. *Biochem. Biophys. Acta.* **1996**, 1295, 147-157.
34. Bailly, C.; Arafa, R. K.; Tanius, F. A.; Laine, W.; Tardy, C.; Lansiaux, A.; Colson, P.; Boykin, D. W.; Wilson, W. D. *Biochem* **2005**, 44, 1941-1952.

## VITA

Raul A. Puente was born in Coahuila, Mexico, on January 26, 1980, the son of Raul Puente Zurita and Rosario Matinez de Puente. After completing his work at John H. Reagan High School, Austin, Texas, in 1999, he entered Austin Community College. In 2002, he transferred to Southwest Texas State University in San Marcos, Texas. He received the degree of Bachelor of Science from Texas State University-San Marcos in December 2004. In January 2005, he entered the Graduate College of Texas State University-San Marcos.

Permanent Address: 1603 J. J. Seabrook Drive

Austin, Texas 78721

This thesis was typed by Raul A. Puente.

